Check for updates

AGU ADVANCING EARTH AND SPACE SCIENCE

Tectonics

RESEARCH ARTICLE
10.1029/2020TC006131

Geochemical and Stratigraphic Analysis of the Chisana Formation, Wrangellia Terrane, Eastern Alaska: Insights Into Early Cretaceous Magmatism and Tectonics Along the Northern Cordilleran Margin

Patrick Manselle[1], Matthew E. Brueseke[1], Jeffrey M. Trop[2], Jeffrey A. Benowitz[3], Darin C. Snyder[4], and William K. Hart[5]

[1]Department of Geology, Kansas State University, Manhattan, KS, USA, [2]Department of Geology and Environmental Sciences, Bucknell University, Lewisburg, PA, USA, [3]Geophysical Institute and Geochronology Laboratory, University of Alaska Fairbanks, Fairbanks, AK, USA, [4]Idaho National Laboratory, Idaho Falls, ID, USA, [5]Department of Geology and Environmental Earth Science, Miami University, Oxford, OH, USA

Key Points:
- Chisana Formation lavas document ~131–117 Ma arc volcanism (e.g., Chisana Arc) along the inboard margin of the accreted Wrangellia terrane
- The Chisana Formation type section documents an upsection transition from subaqueous marine to subaerial depositional processes
- Geochemical compositions are consistent with existing tectonic models that favor east dipping subduction beneath Wrangellia prior to accretion

Supporting Information:
- Supporting Information S1
- Figure S1
- Figure S2
- Table S1
- Table S2
- Table S3
- Table S4
- Table S5

Correspondence to:
M. E. Brueseke,
brueseke@ksu.edu

Citation:
Manselle, P., Brueseke, M. E., Trop, J. M., Benowitz, J. A., Snyder, D. C., & Hart, W. K. (2020). Geochemical and stratigraphic analysis of the Chisana Formation, Wrangellia terrane, eastern Alaska: Insights into Early Cretaceous magmatism and tectonics along the northern Cordilleran margin. *Tectonics*, *39*, e2020TC006131. https://doi.org/10.1029/2020TC006131

Received 11 FEB 2020
Accepted 13 JUN 2020
Accepted article online 16 JUN 2020

Abstract The Chisana Formation consists of Lower Cretaceous volcanic rocks that occur in the Nutzotin Mountains of eastern Alaska. New stratigraphic analysis indicates that the volcanic succession is >2 km thick at the Bonanza Creek type section. We present stratigraphic, geochemical, Sr-Nd-Pb isotope, and U-Pb age data from samples collected from various stratigraphic levels of the Chisana Formation. We demonstrate that the Chisana Formation can be divided into a lower subaqueous unit, a middle transitional unit, and an upper subaerial unit. Chisana Formation lavas range from transitional to subalkaline basalts through andesites. Trace element geochemistry shows high field strength element depletions relative to large ion lithophile elements and hydrous mineral assemblages with calc-alkaline to tholeiitic chemistries, all consistent with a magmatic arc origin. Chisana lavas yield geochemical compositions and isotope characteristics that overlap with magmas from volcanic suites formed within juvenile continental crust and immature island arcs. Volcanism occurred between ~131 and 117 Ma judging from previously reported lava ages and new U-Pb ages of detrital zircons recovered from sandstones that conformably underlie the lowermost Chisana Formation lavas. Our results support existing tectonic models in which an east dipping subduction zone existed beneath Wrangellia during Early Cretaceous time. The upsection shift from marine to terrestrial depositional conditions in the Chisana Formation and the overlying ~117–93 Ma Beaver Lake Formation was coincident with regional shortening. Together, the geologic evidence for shortening and terrestrial deposition are interpreted to reflect accretion/suturing of Wrangellia against inboard terranes.

Plain Language Summary Collision of continental crust and oceanic crust is a fundamental process that results in changes in plate dynamics, creates Earth's largest mountain belts, and changes global climate dynamics by closing ocean basins and raising high topography. In terms of a fundamental and global tectonic process, suturing is on par with oceanic subduction and mid-ocean ridge formation, yet this process remains poorly understood. Our work investigates volcanism that occurred just before one of largest additions of crust to North America over the last 250 million years. The timing of this collision is debated, as is exact location of the colliding oceanic crust prior to collision and what tectonic setting coeval ~131–117 million-year-old volcanism represents. We show that this volcanism formed in a subduction zone and thus demonstrates that an island arc formed on thick crust (relative to modern examples of where island arcs have collided and entwined like Taiwan) was what collided with North America, after closure of a narrow ocean. These results have implications for models that aim to reconstruct how North America formed, as well as for models of the generation of economically significant Cu-Au-Mo mineral deposits in southern Alaska (e.g., Pebble).

1. Introduction

Accretion of allochthonous terranes to continental crust is a fundamental process in the growth of Earth's continents and despite being a global tectonic process, accretion remains poorly understood. The northern

©2020. American Geophysical Union. All Rights Reserved.

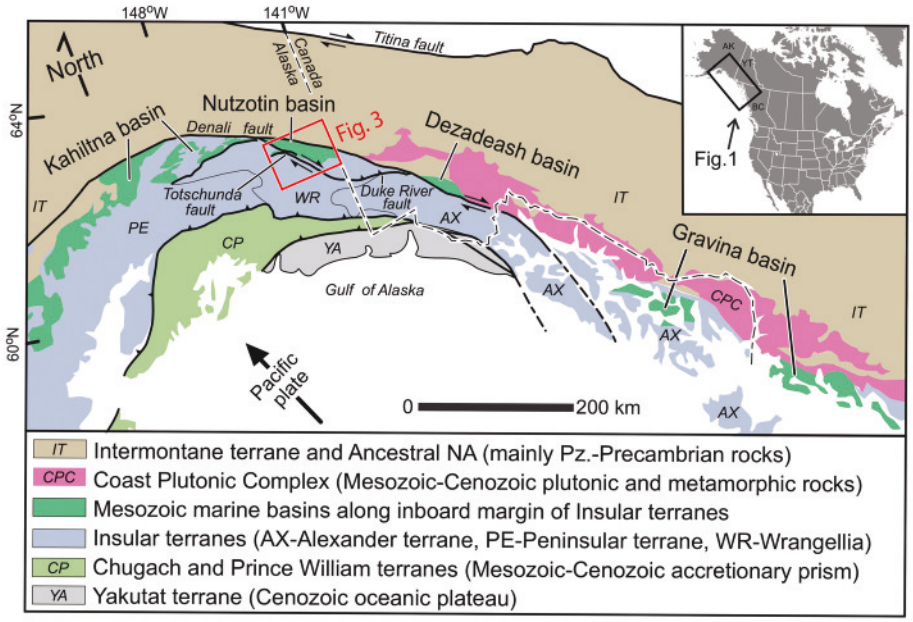


Figure 1. Map (adapted from Trop et al., 2020) showing major terranes and faults along the northern North American Cordillera margin. Marine sedimentary basin deposits (dark green) record accretion of the Insular terranes (Alexander, Wrangellia, and Peninsular terranes—gray) (referred to as the Wrangellia composite terrane in Alaska) against older inboard Intermontane terranes (brown). Red rectangle marks Nutzotin basin focus area shown in Figure 3. Inset map shows location of Figure 1. Abbreviations: AK = Alaska, USA, BC = British Columbia, Canada; YT = Yukon territory, Canada.

Cordillera of western North America is an archetypal example of continental growth through accretionary tectonic processes. A complex collage of allochthonous terranes, sedimentary basins, magmatic belts, and subduction complex strata accreted to inboard terranes during Mesozoic to recent time (e.g., Colpron et al., 2007; Coney et al., 1980; Finzel et al., 2011; Plafker & Berg, 1994). Accretion of the combined Alexander, Wrangellia, and Peninsular terranes (Figure 1) represents one of the largest additions of continental crust to western North America during the past 250 myr. Collectively referred to as the Insular terranes (Colpron et al., 2007), or the Wrangellia composite terrane (Plafker & Berg, 1994), the three terranes amalgamated during late Paleozoic–Mesozoic time, collided with inboard terranes, and shuffled laterally along strike-slip faults (Figure 1) (Gabrielse et al., 2006; Gehrels et al., 2009; Plafker & Berg, 1994; Stamatakos et al., 2001). The timing and location of juxtaposition of the Insular terranes with the inboard terranes varies along strike. Geologic studies in southeastern Alaska suggest juxtaposition occurred initially during mid-Jurassic (McClelland et al., 1992; McClelland & Gehrels, 1990; Monger, 2014; Monger et al., 1994; van der Heyden, 1992) to early Late Cretaceous times (Crawford et al., 1987; Rubin et al., 1990; Rubin & Saleeby, 1991). Geologic studies in south central Alaska indicate initial juxtaposition during Late Jurassic to Early Cretaceous time with final structural accretion during Late Cretaceous time (Box et al., 2019; Hampton et al., 2010; Kalbas et al., 2007; Nokleberg et al., 1994; Stevens Goddard et al., 2018; Trop et al., 2020).

Upper Jurassic–Lower Cretaceous sedimentary and volcanic strata exposed along the inboard margin of the Insular terrane provide a valuable record of tectonic processes. From north to south, these basins are referred to as the Kahiltna, Nutzotin Mountains, Dezadeash, and Gravina basins (Figures 1 and 2), and are commonly referred to as the Gravina-Nutzotin belt (Berg et al., 1972; Plafker & Berg, 1994). Currently, the tectonic setting of these basins is controversial due to uncertainty regarding the timing and location of Insular terrane accretion against the North American paleomargin, as well as the number and polarity of subduction zones associated with this accretionary event. Berg et al. (1972), and most subsequent workers, interpreted the strata to have accumulated along the inboard (eastern) margin of the Insular terranes in a retro-arc position with respect to a west facing subduction system, which is supported by Late Jurassic–Early Cretaceous arc plutons that intrude the Insular terranes, Late Jurassic-Early Cretaceous forearc

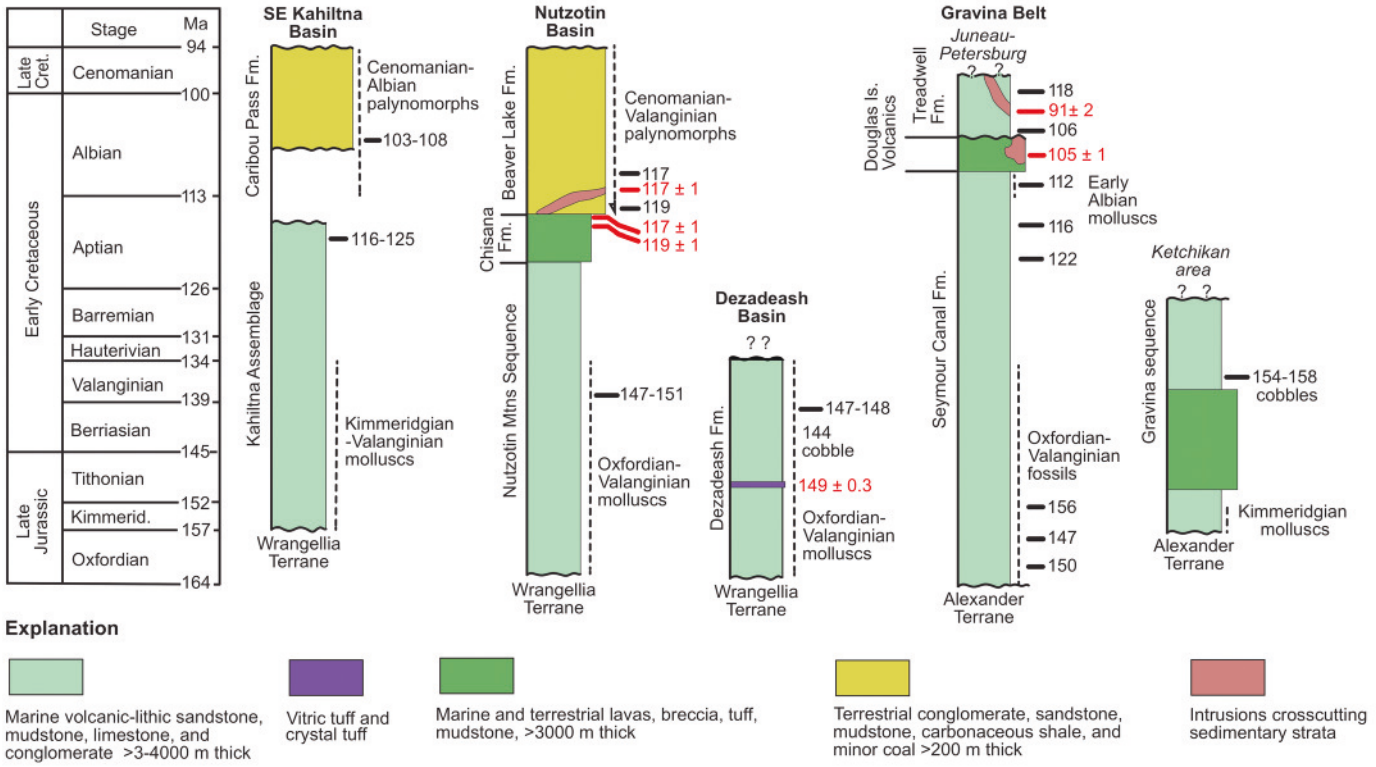


Figure 2. Generalized stratigraphy of Jurassic-Cretaceous basins along the inboard edge of the Insular terranes (adapted from Trop et al., 2020). Refer to Figure 1 for basin locations. Age constraints include fossils (vertical dashed lines), igneous ages (red font), and the youngest populations of detrital zircons (black bold horizontal lines), all in Ma. Data sources: Ketchikan: Rubin and Saleeby (1991), Juneau-Petersburg: Berg et al. (1972), Gehrels (2000), Yokelson et al. (2015), Dezadeash: Lowey (2007, 2011, 2018); Nutzotin basin: Berg et al. (1972), Manuszak et al. (2007), Trop et al. (2020); southeast Kahiltna basin (Talkeetna Mountains): Csejtey et al. (1992), Hampton et al. (2010, 2017). Stratigraphic positions of detrital zircon samples in the Dezadeash basin is estimated.

basin sedimentary strata positioned outboard (south) of the arc plutons, and Late Jurassic-Early Cretaceous marine metasedimentary strata of the Chugach accretionary complex located south of the Insular terranes (Figure 1) (Pavlis et al., 2019; Trop & Ridgway, 2007; Yokelson et al., 2015). Alternatively, some workers attribute basin development and arc magmatism to west dipping subduction beneath the Insular terranes (e.g., Sigloch, 2017).

In addition to debates on the polarity of subduction, interpretations of the tectonic configuration of the Gravina-Nutzotin belt vary considerably, and include the following settings: precollisional oceanic arc (Berg et al., 1972; Lowey, 2018), postcollisional rift or transtensional basin (Gehrels et al., 2009; Kapp & Gehrels, 1998; McClelland et al., 1992), and syncollisional/postcollisional arc (Hampton et al., 2010; Manuszak et al., 2007; Trop et al., 2020). The geochemical character and timing of magmatism (and suturing) between the Insular terranes and North America is also significant for understanding the context for some of the world's largest Cu-Au-Mo porphyry deposits. These deposits and associated ~115 to 75 Ma plutons, which include the Kaskanak batholith and Pebble deposit (Goldfarb et al., 2013), are associated with the suture zone.

Previous studies of the Jurassic–Cretaceous basins exposed along the inboard margin of the Insular terranes have focused chiefly on the sedimentary records. Late Jurassic–Early Cretaceous volcanic rocks are absent in the Kahiltna basin, limited to sparse tuffs in the Dezadeash basin, and intensely deformed/altered in the Gravina basin (Haeussler, 1992; Hampton et al., 2010; Kalbas et al., 2007; Lowey, 2011; Manuszak et al., 2007; McClelland et al., 1992; Stowell et al., 2000; Yokelson et al., 2015). Thus, >2 km thick volcanic successions represented by the Chisana Formation in the Nutzotin basin provide a unique opportunity to evaluate the nature of volcanism along the inboard margin of Wrangellia. Previous geochemical data from Late Jurassic–Early Cretaceous volcanic rocks along the inboard margin of the Insular terranes are limited to

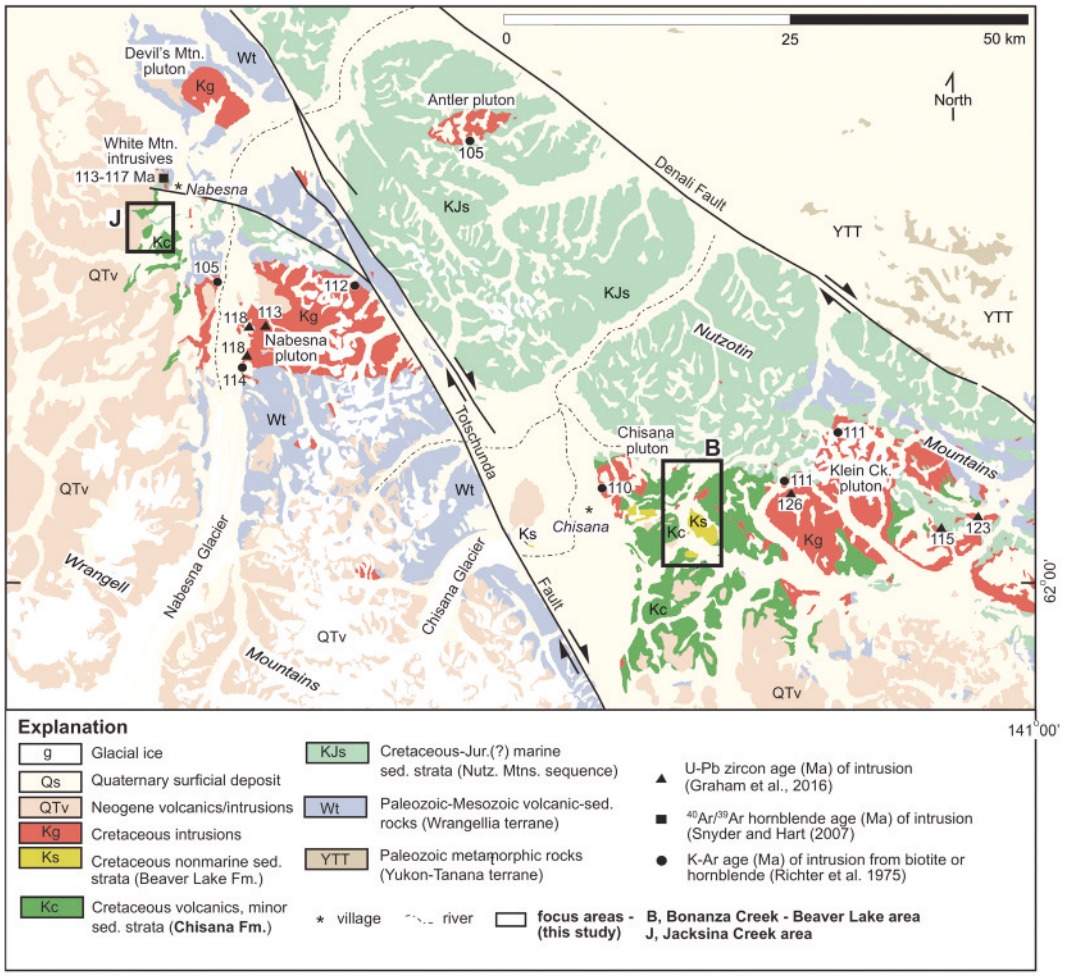


Figure 3. Geologic map of the eastern Alaska Range showing Jurassic-Cretaceous sedimentary, volcanic, and intrusive rocks within the suture zone between the Insular terranes and the Yukon-Tanana terrane (adapted from Trop et al., 2020). Geology adapted from Richter et al. (1976). Refer to Figure 1 for location. Black rectangles mark our two focus areas in the Nutzotin Basin.

19 whole rock geochemical analyses of lavas from the Chisana Formation with no stratigraphic context (Barker et al., 1994), lavas from the Gravina belt (Rubin & Saleeby, 1991; Stowell et al., 2000) and sparse tuffs in the Dezadeash Formation (Lowey, 2011).

This study presents new major and trace element geochemistry, Sr-Nd-Pb isotope constraints, U-Pb detrital zircon geochronology, petrography, and field-based lithologic observations of the Chisana Formation in eastern Alaska (Figures 2 and 3). All data was collected within a stratigraphic context to evaluate possible temporal shifts in magmatism. A detailed discussion of the petrogenesis of Chisana igneous rocks is beyond the scope of this study and not our goal. However, we integrate these new data sets with prior published data from coeval igneous and sedimentary successions, in an effort to elucidate the tectonomagmatic setting of Chisana volcanism. These findings contribute to testable plate tectonic models for the Cordilleran margin during Cretaceous time, including the polarity of subduction, the timing of terrane collision/accretion, and the tectonic setting of sedimentary basins.

2. Geologic Setting

The inboard margin of Insular terranes is juxtaposed against Proterozoic–Paleozoic metamorphic rocks (Yukon-Tanana terrane) and arc-related rocks (Stikine terrane) that are collectively referred to as the Intermontane terrane (Figure 1). The Intermontane terrane accreted to the continental margin by Middle Jurassic time and perhaps much earlier (Beranek & Mortensen, 2011, Foster et al., 1994, Plafker &

Berg, 1994). A zone of complexly deformed Jurassic–Cretaceous sedimentary, igneous and metamorphic rocks separates the Insular and Intermontane terranes (Figure 1) (McClelland et al., 1992). In south central Alaska, the suture zone is defined by the deformed Cretaceous sedimentary strata of the Kahiltna basin, which spans a region as much as 100 km wide that is bordered to the north by the crustal-scale Hines Creek fault and bordered to the south by the Talkeetna fault (Figures 1 and 2) (Brennan et al., 2011; Hampton et al., 2010; Ridgway et al., 2002). In eastern Alaska, a >100 km wide zone of deformation between the Denali fault on the north and the Totschunda fault on the south deforms Cretaceous sedimentary and volcanic strata of the Nutzotin basin and the underlying Wrangellia terrane (Figures 1 and 2; Allam et al., 2017; Manuszak et al., 2007; Richter, 1976; Trop et al., 2020). In Yukon, deformed Cretaceous sedimentary strata that are dextrally displaced from the Nutzotin basin crop out north of the Denali fault (Dezadeash basin on Figures 1 and 2) (Lowey, 2018). In southeastern Alaska, the zone is characterized by known and inferred, mid-Cretaceous inboard- (east) dipping thrust faults, shear zones, and intrusions that deform Jurassic–Cretaceous sedimentary and volcanic strata of the Gravina basin (Figures 1 and 2) (Crawford et al., 1987; Gehrels et al., 1992 ; Rubin & Saleeby, 1991).

The outboard margin of the Insular terranes is juxtaposed against the Chugach and Prince William terranes (Figure 1), which consist of Jurassic–Cretaceous oceanic sedimentary and volcanic rocks interpreted as subduction complex deposits associated with northeastward/eastward subduction (modern coordinates) beneath the Insular terranes (e.g., Amato et al., 2013). The magmatic record of subduction includes plutons and subordinate volcanic rocks within the Insular terranes that represent the remnants of magmatic arcs that range in age from Pennsylvanian to Late Cretaceous (Moll-Stalcup, 1994; Plafker & Berg, 1994). In south central and eastern Alaska, these igneous successions are referred to as the Early to Late Jurassic Talkeetna arc, the Late Jurassic to Early Cretaceous Chitina arc, and the late Early Cretaceous Chisana arc (Plafker & Berg, 1994). In southeastern Alaska and north coastal British Columbia, Jurassic–Cretaceous arc plutons intruding the Insular terranes are referred to as the western Coast Mountains batholith (Cecil et al., 2011, 2018; Gehrels et al., 2009); in southwestern Yukon and northwestern British Columbia they are the Saint Elias plutonic suite (Beranek et al., 2017).

Upper Jurassic to Lower Cretaceous sedimentary and volcanic strata up to 6 km thick overlie the inboard (northern) margin of Wrangellia in the Nutzotin Mountains (Figures 1–3) (Manuszak et al., 2007; Richter, 1976). Referred to as the Nutzotin basin, the succession consists of three distinct stratigraphic units: a lower marine sedimentary succession, a middle volcanic succession, and an upper terrestrial sedimentary succession. The lower succession consists of the Nutzotin Mountains sequence, a >3 km thick sequence of Upper Jurassic to Lower Cretaceous sandstone, conglomerate, and mudrock that depositionally overlies Triassic sedimentary strata of Wrangellia (Berg et al., 1972; Manuszak et al., 2007; Richter, 1976). Marine fossils indicate that deposition spanned Late Jurassic (Oxfordian) to Early Cretaceous (Valanginian) time and lithofacies reflect deposition mainly in submarine slope/fan environments (Berg et al., 1972; Manuszak et al., 2007). U-Pb detrital zircon ages from the Nutzotin Mountain sequence display unimodal populations between ~155–133 Ma; the stratigraphically youngest strata yield a unimodal ~128–119 Ma detrital zircon age peak (Fasulo, 2019). Paleocurrents, conglomerate clast compositions, and detrital zircon ages from the Nutzotin Mountains sequence indicate erosion of local sources within Wrangellia and northward to northeastward sediment transport (Fasulo et al., 2018; Manuszak et al., 2007).

Depositionally overlying the Nutzotin Mountains sequence is the Lower Cretaceous Chisana Formation (Figure 4), the focus of this study. The Chisana Formation consists of a >3 km thick succession of lavas, volcanic breccia, volcaniclastic sandstone, tuff, and mudstone (Berg et al., 1972; Manselle, 2019; Richter & Jones, 1973; Short et al., 2005). The Chisana Formation has a gradational depositional contact with Nutzotin Mountains sequence strata that bear Valanginian marine fossils (Manuszak et al., 2007; Richter & Jones, 1973). Chisana Formation volcanic rocks accumulated during Early Cretaceous time judging from Hauterivian-Barremian (~133–125 Ma) marine fossils in the lower ~500 m of the Chisana Formation (Berg et al., 1972; Sandy & Blodgett, 1996) and ~122–116 Ma $^{40}Ar/^{39}Ar$ cooling ages from lavas in the upper half of the Chisana Formation (Trop et al., 2020). Surrounding and locally crosscutting the volcanic strata are intrusions that yield ~126–113 Ma U-Pb zircon crystallization ages (Figure 3) (Graham et al., 2016) and ~117–113 Ma $^{40}Ar/^{39}Ar$ cooling ages (Snyder & Hart, 2007). These intrusions are locally associated with coeval Cu-Au-Mo porphyry mineralization (e.g., Nabesna, Orange Hill, Baultoff, Carl Creek, Horsfeld, Chisana deposits) (Graham et al., 2016).

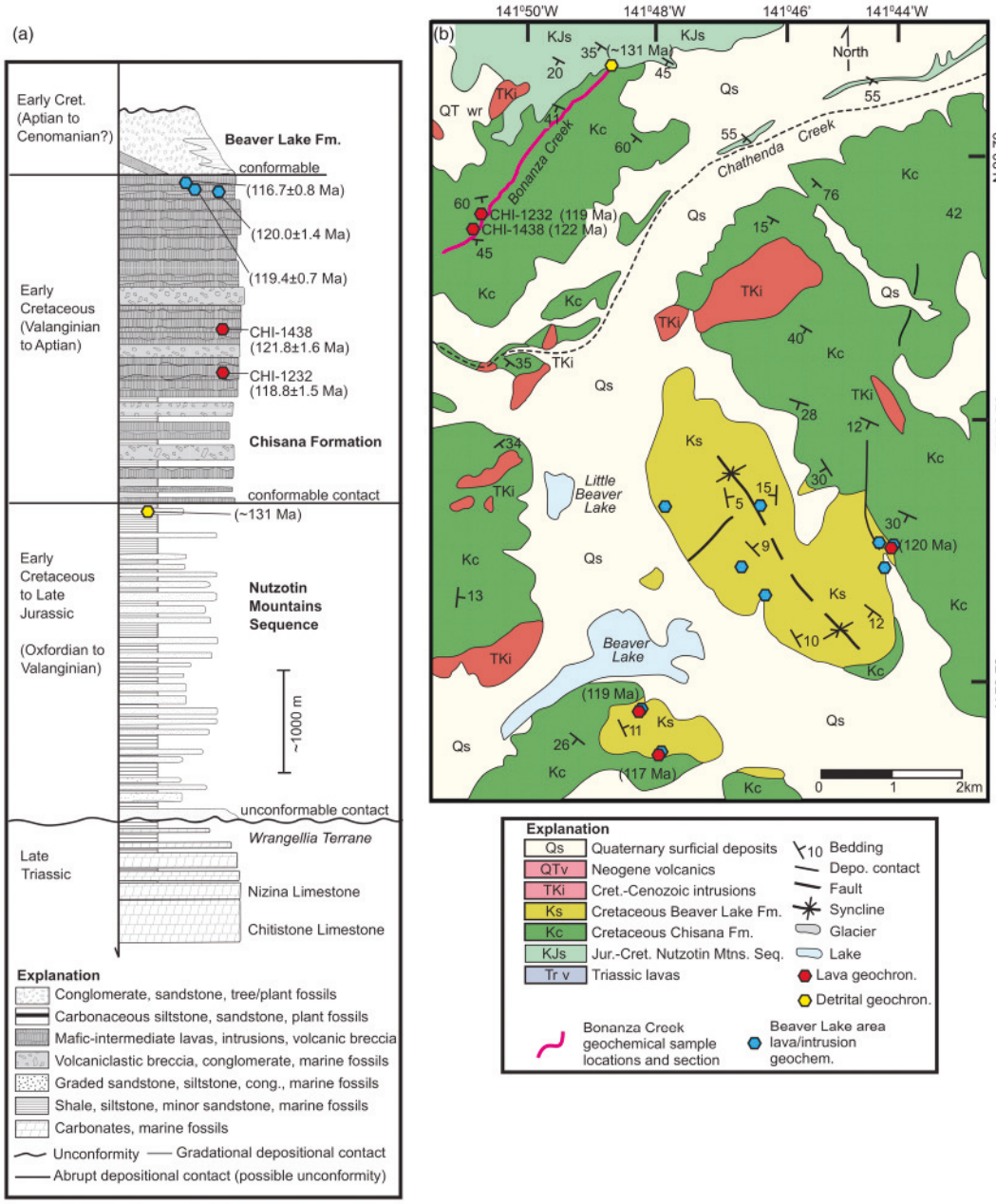


Figure 4. Generalized stratigraphy (a) and geologic maps of the Bonanza Creek-Beaver Lake focus area (b), showing sample locations and Bonanza Creek measured stratigraphic section (adapted from Trop et al., 2020). Geology from Richter (1971) and Richter and Jones (1973). *X* axis in (a) depicts weathering profile. Refer to Figure 3 for location.

Depositionally overlying the Chisana Formation is a >200 m thick succession of sedimentary strata referred to as the Beaver Lake formation (Figure 4; Trop et al., 2020). Strata of the Beaver Lake formation include conglomerate, sandstone, and mudrock with well-preserved plant fossils and dinosaur footprints that accumulated in fluvial environments (Fiorillo et al., 2012; Trop et al., 2020). Fluvial deposition commenced by ~117 Ma and ceased by ~98 Ma judging from palynomorphs, the youngest detrital zircon ages, and the ages of cross-cutting intrusions and underlying lavas of the Chisana Formation (Trop et al., 2020).

3. Sampling Strategy and Methods

Our analysis of the Chisana Formation is based on field work at three focus areas, Bonanza Creek, Beaver Lake, and Jacksina Creek, previously mapped by Richter (1976) and Löwe et al. (1982). Figures 3–5 show

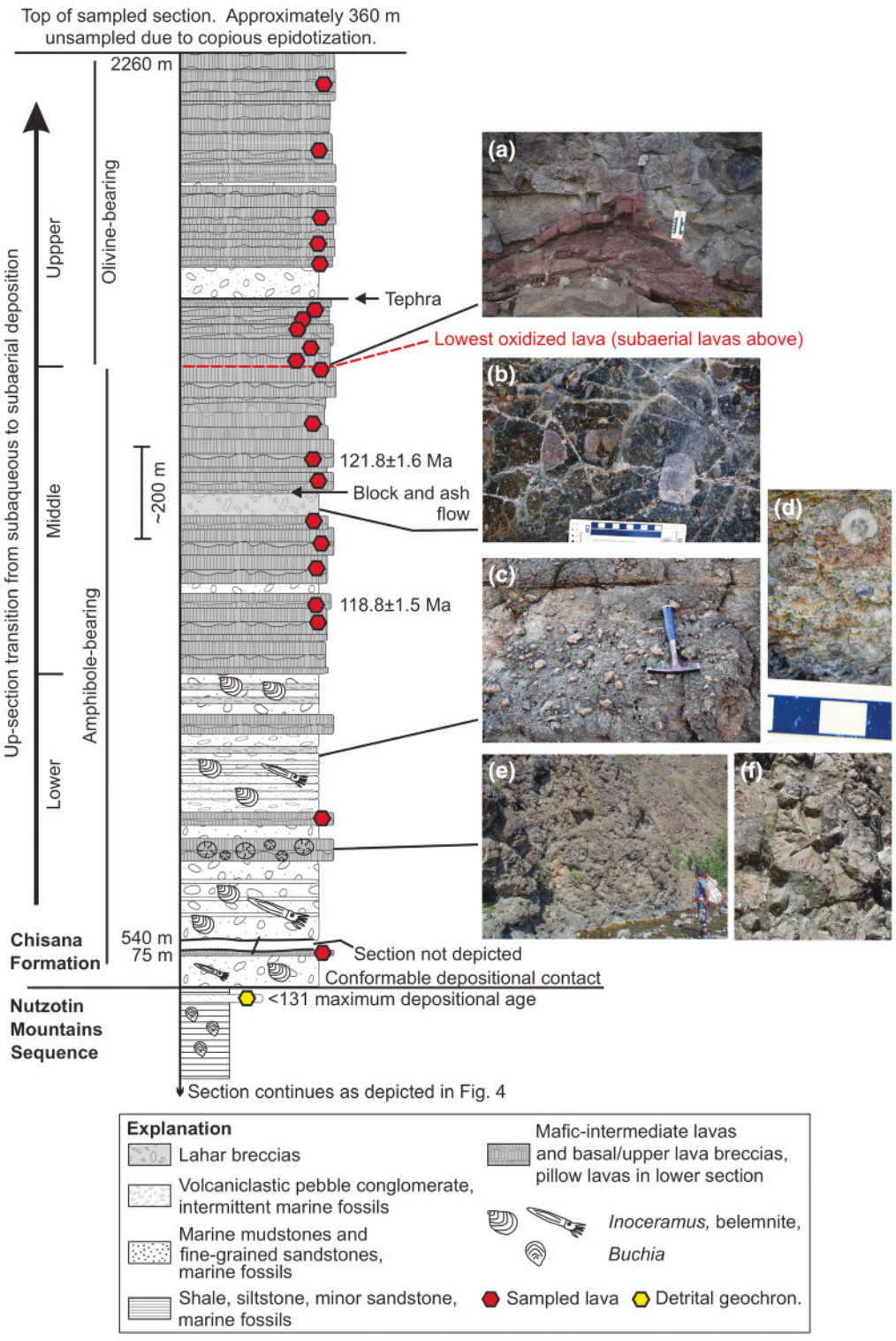


Figure 5. Chisana Formation stratigraphy at Bonanza Creek (Figure 3). Refer to Manselle (2019) for additional stratigraphic details. (a) Contact of first oxidized lava autobreccias (basalt autobreccia above red oxidized contact marking the base of subaerial lava facies. (b) Lahar breccia with sedimentary and volcanic clasts. (c) Volcaniclastic conglomerate facies; very poorly sorted, with pebble sized clasts and coarse sand-sized matrix. Clasts are volcanic in nature and are texturally consistent with derivation from underlying lavas (~28 cm rock hammer for scale). (d) Cross section of belemnite fossil in volcaniclastic conglomerate. (e) Lower Chisana Formation pillow lavas; person ~1.7 m tall. (f) Close-up of pillow in (e). Note the diagnostic radial fractures and vesicles adjacent to quenched margin.

the generalized stratigraphy and geologic maps with sample locations and a measured stratigraphic section for the Bonanza Creek and Beaver Lake areas. Refer to Figure S2 in the supporting information for a geologic map of the Jacksina Creek area. Lithologies were grouped into lithofacies on the basis of grain size, sedimentary structures, fossils, and volcanic structures. Thirty-five samples (this study) were collected from sedimentary and igneous strata in 2016 and 2018. This suite includes nine samples collected from Chisana lavas and dikes in outcrops along the north and east margins of Beaver Lake (Figures 3 and 4); their physical characteristics and relationships with sedimentary strata of the overlying Beaver Lake formation strata are presented in Trop et al. (2020). Only the freshest rocks were targeted for collection. Thin sections were used for mineral and textural characterization and to determine the extent of alteration for selection of samples for geochemical analyses. Photomicrographs of representative samples are found in Figure S1. Twenty-seven samples were then selected for geochemical analyses based on the lack of obvious postemplacement alteration in hand sample and thin section and after applying an alteration filter (Beswick & Soucie, 1978) (refer to Table S2 in the supporting information for methods). These new samples extend the stratigraphic range of a suite of 16 samples previously collected in 2001 from the lower and middle sections of the Chisana Formation stratigraphy at Bonanza Creek (Short et al., 2005); data from the previously collected 16 samples were never published but are reported here. Overall, bulk rock geochemical compositions from 43 total samples are reported here. Total volatiles loss on ignition (LOI) were determined for each sample. Major elements are reported as wt.% oxide and trace element concentrations are presented as parts per million (ppm). All major, trace, and rare-earth element (REE) data are presented in Table S2. Fe was split according to Le Maitre (1976) and all major element data used in diagrams and the discussion are reported as anhydrous using the split Fe data.

A subset of lavas from Bonanza Creek were selected for Sr, Pb, and Nd isotopic measurements. Isotopic compositions were measured by thermal ionization mass spectrometry (TIMS) at Miami University, using a Finnigan Triton mass spectrometer. Isotope separation techniques, analytical methods, and analytical errors, and Sr-Nd-Pb data are reported in the supporting information (Table S3). Sr and Nd isotope ratios are reported age-corrected to 120 Ma, which represents the mean age of lava emplacement based on new detrital geochronologic ages from the base of the Chisana Formation at Bonanza Creek (Figure 4), previously reported Chisana lava and dike ages (Trop et al., 2020), and previously reported ages from intrusions that crop out among the Chisana volcanics (Figure 3) (Graham et al., 2016; Snyder & Hart, 2007).

Sandstones from the upper part of the Nutzotin Mountains sequence were sampled for detrital zircon geochronology to provide additional constraints on the age of the volcanic succession. A sandstone was sampled directly below the lowermost lava flow at Bonanza Creek. Two sandstones were also collected from outcrops underlying the volcanic strata along Jacksina Creek (Figure S2). Zircon separation was performed using standard methods, including crushing/pulverizing, followed by separation with a Wilfley table, Frantz magnetic separator, and heavy liquids. Grains were mounted in a 2.54 cm epoxy mount alongside fragments of standard zircons. Laser Ablation Inductively Coupled Plasma Mass Spectrometry (LA-ICP-MS) data collection was performed by Dr. P. O'Sullivan at GeoSep Services in Moscow, Idaho. Analytical details and a summary table of detrital zircon U-Pb ages is found in the supporting information (Table S1).

4. Results

4.1. Sedimentary and Volcanic Lithofacies

Physical volcanic and sedimentologic observations were made from outcrops at Bonanza Creek, Beaver Lake, and Jacksina Creek (Figure 3). Lithofacies observed in the Chisana Formation and the uppermost part of the Nutzotin Mountains sequence at these locations are summarized below. All lithofacies are observed at the ~2.25 km thick section of Chisana Formation along Bonanza Creek (Figures 4a and 5). We subdivided the stratigraphy at Bonanza Creek into lower, middle, and upper sections based on the distribution of lithofacies.

4.1.1. Nutzotin Mountain Sequence at Bonanza Creek

This unit depositionally underlies the Chisana Formation at Bonanza Creek. At Bonanza Creek, this facies consists of gray mudstone and shale with subordinate normal-graded fossiliferous sandstone, conglomerate,

and limestone. This facies is interpreted to represent subaqueous marine deposition between fair weather and storm wave base. Mudstones accumulated by suspension fallout during fair-weather conditions whereas coarser grained sandstones and conglomerates were deposited by combined flow and sediment gravity flow (Manuszak et al., 2007; this study).

4.1.2. Nutzotin Mountains Sequence at Jacksina Creek

Sedimentary strata underlying the Chisana Formation at Jacksina Creek consist of fine-grained sandstone, mudrock, carbonaceous shale, and coal that preserve symmetrical ripple cross-stratification, flaser bedding, lenticular bedding, wavy bedding, and rootlets (Figure S1). Heterolithic strata composed of finely laminated sandstone and mudstone and carbonaceous strata occur locally. Carbonaceous strata, mainly coal and carbonaceous shale are common, and contain abundant comminuted organic debris and well-preserved plant fossils. This facies is interpreted to represent subaerial and subaqueous deposition by a combination of fluvial, tidal, and wave processes in vegetated coastal environments and is strikingly different than the Nutzotin Mountains Sequence at Bonanza Creek. New detrital zircon U-Pb ages from these terrestrial strata yield <131 Ma maximum depositional ages (Figure S2 and Table S1).

4.1.3. Marine Mudstones and Minor Fine-Grained Volcanic-Lithic Sandstone

This facies only occurs in the lower section of the Chisana Formation at Bonanza Creek. It consists of mudstone, siltstone, and subordinate fine-grained to very fine grained lithic sandstone in the lower Chisana Formation and the upper part of the Nutzotin Mountain sequence. These strata yield marine fossils, including brachiopods (Sandy & Blodgett, 1996) and Buchia bivalves (Richter et al., 1975). Most brachiopods and bivalves are disarticulated and abraded, although articulated unabraded specimens occur locally. Sandstones are sharp-based, ungraded to normal-graded with fossiliferous bases locally. This lithofacies reflects subaqueous marine deposition between fair weather and storm wave base. Mudstones reflect suspension fallout during fair-weather conditions, whereas sandstones indicate combined flow during episodic storms.

4.1.4. Volcaniclastic Conglomerate

This facies only occurs throughout the lower and middle parts of the Chisana Formation at Bonanza Creek. It consists of green, volcaniclastic, matrix-supported granule to pebble conglomerate that represents the thickest facies in the lower section of the Chisana Formation at Bonanza Creek and is present throughout the entire formation. Clasts are a mixture of volcanic and sedimentary rocks. Clasts are typically rounded to subrounded and poorly sorted, with a maximum clast size of ~50 cm. Volcanic clasts are petrographically similar to mafic-intermediate Chisana lavas that are interbedded with this facies. In the lower section of the Chisana Formation, these deposits contain marine fossils, mainly belemnites and *Buchia* and *Inoceramus* bivalves (Figure 5). Thickness of this facies ranges from ~8 to ~180 m. The parts of this facies that are in the lower section of the Chisana Formation at Bonanza Creek are frequently cut by mafic dikes. In a single location in the upper section at Bonanza Creek (Figure 5), this facies also contains thinly bedded (<6 cm thick) tephras that are interbedded with the volcaniclastic conglomerate. This lithofacies implies subaqueous deposition via primary volcanic processes and mass wasting onto the flanks of active volcanoes. Volcaniclastic strata were deposited in a subaqueous marine environment judging from the marine fossils and interbedded pillow lavas (described below). Similar volcaniclastic strata occur in the Jurassic–Cretaceous basinal strata along the inboard margin of the Insular terranes, including the Talkeetna arc (Clift, Pavlis, et al., 2005; Draut & Clift, 2006) and the Gravina belt (Rubin & Saleeby, 1991). Interbedded with Jurassic–Cretaceous marine sedimentary strata in the Dezadeash basin are sparse tuffs (Lowey, 2011) that may represent distal products of these strata.

4.1.5. Marine Lavas

Stratified basaltic andesite to basaltic lavas typify this lithofacies that is only observed at Bonanza Creek. Most lavas are massive, though units up to 50 m thick with pillow structures >1.1 m long occur in the lower part of the Bonanza Creek section (~699 to ~747 m on Figure 5). Lavas are porphyritic, with fine-grained, gray matrices and phenocrysts of plagioclase, pyroxene, and amphibole. Plagioclase phenocrysts are more abundant than pyroxene phenocrysts, typically comprising ~60–80% modally, whereas pyroxene typically makes up ~5–10%. Autobrecciated lava tops and bottoms are present in marine lavas in the middle section of the Chisana Formation. Lavas are interbedded with volcaniclastic conglomerates and mudstones containing marine fossils from the volcaniclastic conglomerate and marine mudstone facies, which imply marine deposition of the lavas. This facies represents a subaqueous marine environment judging from the pillow structures in lavas and from marine fossils in adjacent sedimentary strata.

4.1.6. Lahar Breccias

Inversely graded, poorly sorted, and mudstone matrix-supported breccias define this facies, which occurs in the lower and middle portions of Bonanza Creek and also at Jacksina Creek. Clasts are angular to subrounded and poorly sorted, and consist of lithologies that match underlying volcanic and sedimentary rocks within the Chisana Formation (Figure 5). The mean clast size is ~8 cm. Clasts are more angular than clasts within volcaniclastic conglomerate. The mudstone matrix, poor sorting, and angular nature of clasts typify lahar breccias (Compton, 1985). This facies reflects debris flow and flood flow deposition on volcanic aprons flanking an active volcano (e.g., Trop et al., 2012).

4.1.7. Block and Ash Deposit

This lithofacies is only found in the middle portion of Bonanza Creek and consists of a gray-green mudstone matrix-supported volcaniclastic pebble conglomerate. Clasts are poorly sorted, and composed primarily of subangular welded tuff up to 15 cm in length. The presence of welded tuff clasts in this unit indicates the presence of elevated (relative to the area they were deposited in) lava domes that collapsed and produced pyroclastic density currents.

4.1.8. Oxidized Lavas

This lithofacies is characterized by the presence of reddish brown, oxidized lavas with autobrecciated tops and/or bottoms (Figure 5). These locally vesicular and massive lavas occur in the upper Chisana Formation at Bonanza Creek, throughout the Chisana Formation at Jacksina Creek, including lowermost lavas that directly overlie the Nutzotin Mountain Sequence at Jacksina Creek, and at Beaver Lake. In these locations, lavas occur as thick packages that are distinguishable by autobreccias in interflow zones. These lavas are porphyritic with plagioclase, pyroxene, olivine, and amphibole phenocrysts, occasional plagioclase-clinopyroxene glomerocrysts, and typically contain 50–60% plagioclase, 0–24% pyroxene, and contain relict olivine phenocrysts, in a trachytic groundmass. The evidence of oxidation in the lava tops/bottoms indicates effusive eruptions in a subaerial environment.

4.2. Petrography of Chisana Lavas

Most lava hand samples are light to dark gray in color, exhibit trachytic texture, and are often porphyritic (Figure S1). Phenocrysts of plagioclase, 1–3 mm in size, are present in most, with many samples also containing 1–4 mm pyroxene crystals. Plagioclase is the dominant phenocryst phase for all samples, is typically altered, and exhibit sieve textures and zonation. Olivine pseudomorphs are present only in samples from Jacksina Creek and the upper section of the Chisana Formation at Bonanza Creek. Clinopyroxene is the dominant mafic phenocryst found in samples from the upper and lower sections of the Chisana Formation at Bonanza Creek. Orthopyroxene is typically less abundant than clinopyroxene. Pyroxene phenocrysts range in size from over 4 mm to microcrystalline. Many pyroxene phenocrysts exhibit twinning, and form glomerocrysts. Amphibole is only present in samples from the lower and middle sections at Bonanza Creek and from samples at Jacksina Creek. The groundmass of the lavas and dikes contain intersertal plagioclase laths, pyroxene crystals, opaque minerals, serpentine, chlorite, zeolites, sericite, kaolinite, and epidote. Chisana Formation lavas are locally amygduloidal, with vesicles filled by epidote, zeolites, serpentine, and calcite. Alteration is discernable as pyrite blebs, veins of carbonates and sulfides, and as replacement of primary minerals by serpentine, epidote and other secondary alteration minerals (Manselle, 2019).

4.3. Geochemical Classification and Bulk Rock Geochemical Characteristics

On the total alkalis versus silica diagram (Le Bas et al., 1986), the samples from Beaver Lake, Bonanza Creek and Jacksina Creek are classified as transitional basalts to andesites, with SiO_2 values ranging from 44.7 to 63.4 wt.% (Figure 6a). The incompatible element-based classification scheme of Pearce (1996) yields similar names. The similarity in classification using the two different schemes suggests that alteration has had a relatively small effect on the bulk chemical composition (Figure 6b). On an alkali-FeO*-MgO (AFM; where FeO* is the total Fe expressed as FeO) diagram (Figure 6c), samples from the upper Chisana Formation at Bonanza Creek follow a tholeiitic array whereas samples from middle and lower portions, Beaver Lake, and Jacksina Creek dikes plot along a calc-alkaline array. Most of the Jacksina Creek lavas plot along a tholeiitic array. All sampled Chisana lavas are also characterized by enrichment of LILE (large ion lithophile elements) and depletion of HFSE (high field strength elements) relative to each other (Figure 7), which are characteristic elemental enrichments and depletions associated with magmas produced in subduction

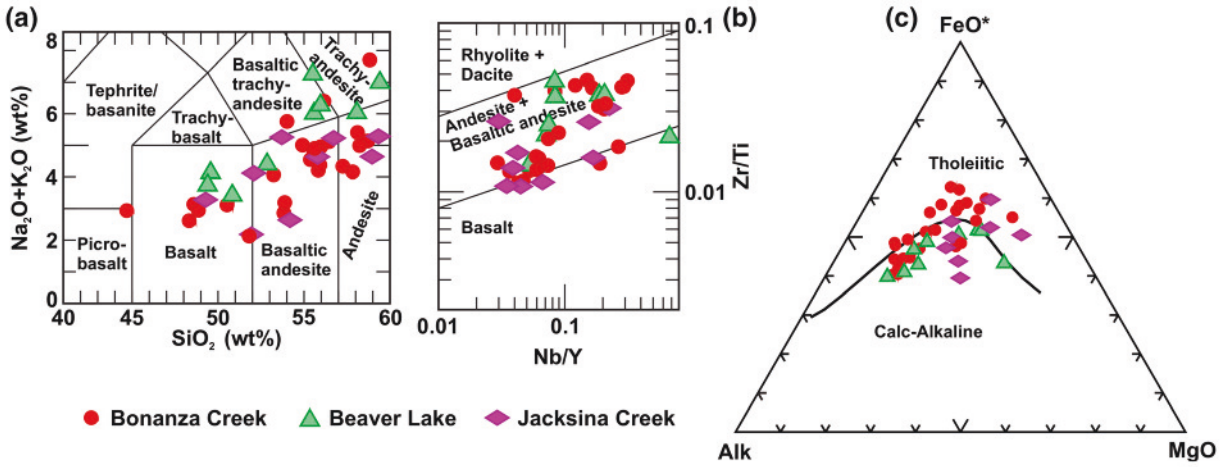


Figure 6. Geochemical classification diagrams. (a) Volcanic rock classification diagram based on Le Bas et al. (1986). Chisana Formation igneous rocks are composed primarily of basalts, basaltic andesites, and andesites/trachyandesites and are transitional to subalkaline. (b) Zr/Ti versus Nb/Y rock classification scheme after Pearce (1996). (c) AFM diagram after Irvine and Baragar (1971), shows that Chisana Formation igneous rocks have tholeiitic to calc-alkaline affinities. Refer to Figures 3, 4, and S2 for sample site locations.

environments. Other trace elements also show subduction influence; for example, a plot of La versus Nb (Figure 8a) shows that Chisana samples are characterized by La enrichment and Nb depletion, consistent with melting of subduction-affected mantle (Pearce & Peate, 1995). Chisana lavas studied here are also geochemically similar (e.g., light rare-earth element [LREE]-enriched, La/Yb = 2.6 to 12.1) to igneous rocks sourced primarily in the rear arc segment (also LREE-enriched; La/Yb > 2.2) of the Izu-Bonin arc (Figure 8b), an archetypal example of an extensional, intra-oceanic magmatic arc (Ducea et al., 2015; Morris et al., 2019; Stern, 2010).

4.4. Sr-Nd-Pb Radiogenic Isotope Characteristics

Figures 9a and 9b depict the age-corrected (to 120 Ma) $^{87}Sr/^{86}Sr_i$ and εNd_i values of a representative suite of Chisana lava samples from Bonanza Creek. $^{87}Sr/^{86}Sr_i$ values range from 0.702899 to 0.703163 and εNd_i also spans a small range from +8.39 to 8.72. The sample suite defines an array that extends to slightly more radiogenic $^{87}Sr/^{86}Sr_i$ values as εNd_i slightly decreases. Pb isotope values show more variation (Figure 9c), where $^{206}Pb/^{204}Pb$ = 18.533 to 19.079, $^{207}Pb/^{204}Pb$ = 15.491 to 15.525, and $^{208}Pb/^{204}Pb$ = 37.921 to 38.260. They have similar Pb isotope characteristics as prior published Chisana lavas (Aleinikoff et al., 2000) and extend toward more radiogenic values that characterize similarly-aged Nutzotin basin plutonic rocks (Graham et al., 2016) (Figure 9c). Furthermore, the least radiogenic Chisana lavas from this study possess a greater component of MORB mantle in their Pb isotope characteristics than other similarly aged regional igneous products (Figure 9c).

5. Discussion

5.1. Stratigraphic Relationships

Lithofacies analyses of the Chisana Formation document temporal and spatial variations in depositional conditions. The Chisana Formation at Bonanza Creek records an upsection transition from subaqueous deposition and eruptions to subaerial deposition and eruptions. The presence of marine fossils and pillow lavas in the lower section of the Chisana Formation, along with the inferred depositional setting of the underlying Nutzotin Mountains sequence (Berg et al., 1972; Manuszak et al., 2007; Richter, 1976; this study) support a marine environment. The middle section at Bonanza Creek contains a much higher proportion of lavas compared to the lower section and is interpreted to represent a transition between subaqueous and subaerial deposition. Marine fossils indicate that some of the sedimentary strata in the middle section of the Chisana Formation at Bonanza Creek accumulated in marine environments. Overall sedimentary strata decrease in abundance upsection as volcanic strata increase. The upper part of the Chisana Formation at Bonanza Creek, with its massive, oxidized lavas represents primarily subaerial deposition/emplacement.

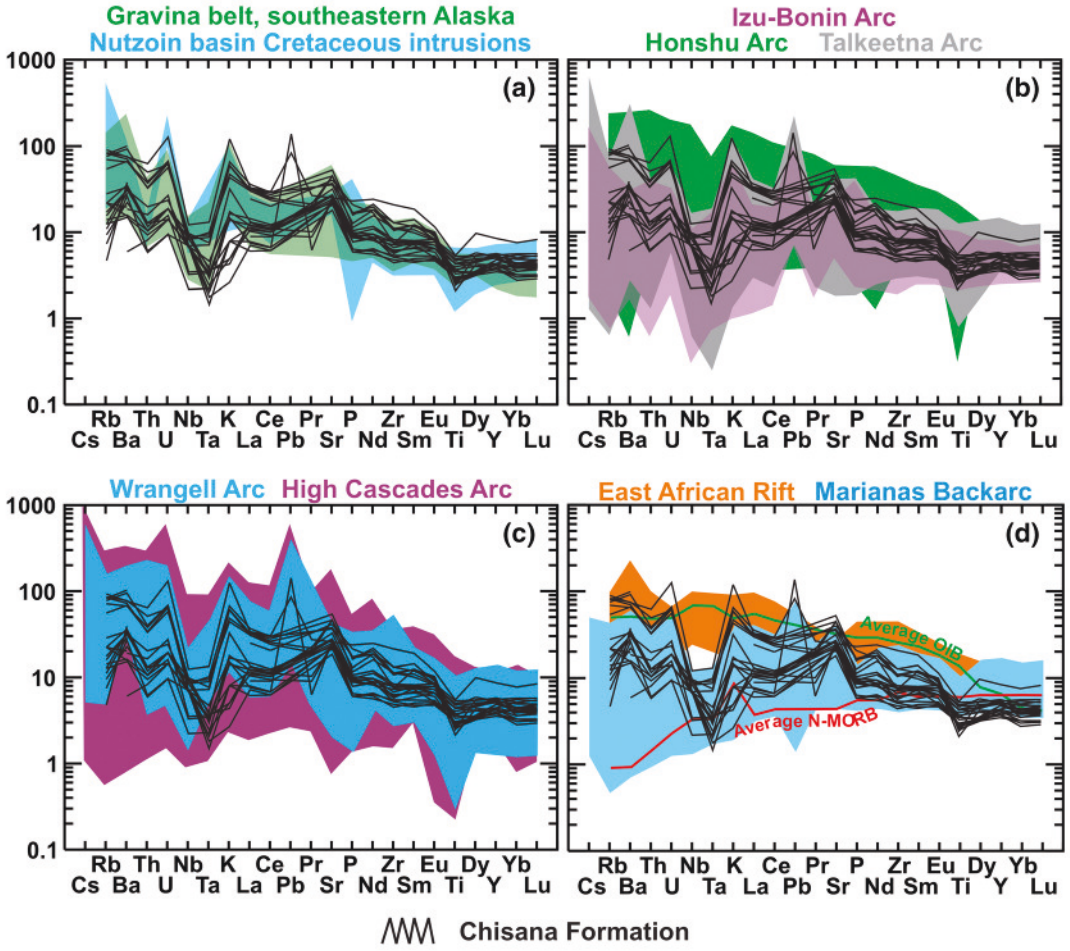


Figure 7. Primitive mantle normalized multielement diagrams comparing Chisana samples with REE data (black lines; Barker et al., 1994 and this study) to other rock suites. Normalizing values from Sun and McDonough (1989). Overall, LILE enrichments and HFSE depletions relative to other elements are present in the Chisana rocks, which is typical of arc magmatism. (a) Nutzotin basin Cretaceous intrusions (Richter et al., 1975; Snyder & Hart, 2007) and metabasalts from the Gravina Sequence (Figures 1 and 2; McClelland et al., 1992; Rubin & Saleeby, 1991; Stowell et al., 2000. (b) Island arcs—Talkeetna arc, Alaska (Clift, Draut, et al., 2005); Japanese Honshu arc ($n = 181$, GEOROC database); Izu-Bonin arc ($n = 80$; Tollstrup et al., 2010). (c) Continental arcs—Wrangell Arc, Alaska (Berkelhammer et al., 2019; Brueseke et al., 2019; Preece & Hart, 2004); High Cascades ($n = 874$, GEOROC database). (d) Igneous rocks from the East African rift (Giordano et al., 2014) and Marianas backarc ($n = 61$, Pearce et al., 2005). For comparison, average OIB-ocean island basalt and normal mid ocean ridge basalts (N-MORB; Sun & McDonough, 1989) are also illustrated.

Chisana lavas that crop out directly below the Beaver Lake Formation at the nearby Beaver Lake area (Figure 3) lack evidence of a subaqueous (marine) eruptive environment.

Observations of the Nutzotin Mountains sequence at the Jacksina Creek locality, indicate deposition in a coastal environment influenced by fluvial, tidal, and wave processes prior to Chisana volcanism (Figure S1). The Chisana Formation at Jacksina Creek consists of oxidized lavas and autobrecciated lava tops/bottoms interbedded with the volcaniclastic conglomerate facies (Figure S1). The lavas and sedimentary strata at Jacksina Creek are physically and chemically identical to the oxidized lavas and conglomerates from the upper section at Bonanza Creek attributed to subaerial deposition/emplacement. The observed stratigraphic relationships are consistent with an inboard- (northeast) dipping depositional gradient along the outboard (southwestern) margin of the Nutzotin basin. Moreover, the upsection transition from marine to terrestrial conditions likely reflects progradation of volcanic flanks during growth of eruptive centers (e.g., Trop et al., 2012), crustal shortening, and/or sea level lowering (discussed below).

5.2. Geochemical and Radiogenic Isotope Constraints on Chisana Formation Magmatism

New analyses reported in this study, in addition to existing published data from Chisana lavas (Barker et al., 1994) and plutons (Richter et al., 1975; Snyder & Hart, 2007), provide strong evidence that the

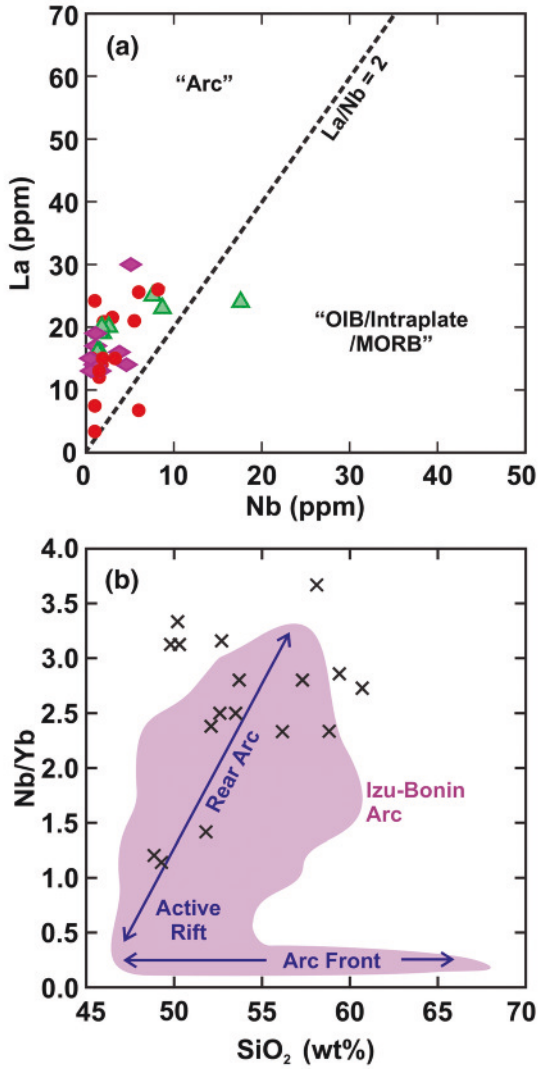


Figure 8. (a) Nb versus La tectonic discrimination diagram (after Brueseke et al., 2019). Chisana Formation samples from this study plot primarily in the "arc" field, consistent with subduction depletion of high-field strength elements like Nb. Symbols as in Figure 6. (b) SiO_2 versus Nb/Yb (after Morris et al., 2019) comparison of Chisana Formation samples (this study and Barker et al., 1994 = black "X") to Izu-Bonin arc eruptive products (n = 463; DeBari et al., 2020; Tollstrup et al., 2010).

Chisana Formation and associated intrusions reflect arc magmatism. As mentioned, subduction processes produce magmas that are enriched in LREEs and LILEs and depleted in heavy rare-earth elements (HREEs) and HFSEs (Smithies et al., 2007); these characteristic enrichments and depletions are present in nearly all samples from the Chisana Formation (Figure 7). Figure 7 also illustrates how Chisana lavas compare to other local igneous rock suites within the Insular terranes, as well as well-studied suites of arc rocks from active oceanic and continental settings. Chisana lavas have nearly identical primitive mantle normalized patterns as broadly contemporaneous igneous belts emplaced along the inboard margin of the Insular terranes (Figures 1, 2, 3, 7). These data support previous hypotheses that Early Cretaceous plutons in the Nutzotin basin are petrogenetically related to Early Cretaceous Chisana lavas (Snyder & Hart, 2007) and that these are part of the same volcanic arc that presently crops out for >2,000 km from south central to southeastern Alaska and coastal British Columbia (Gehrels et al., 2009; Plafker & Berg, 1994).

Chisana lavas have similar chemical compositions as other island arcs (Figure 7b). For example, Chisana lavas have similar overall enrichments and depletions when compared to the modern Honshu arc (Japan), a possible modern proxy, and also the Jurassic Talkeetna arc (Alaska; Clift, Draut, et al., 2005). The similarity with Talkeetna rocks is to be expected, as the suites of igneous rocks both represent arc magmatism within the Insular terranes, albeit at different times. Figures 7d and 8b also illustrate the similarity of Chisana lavas to Izu-Bonin arc magmatism, especially with the Izu-Bonin rear-arc segment. Figure 7c illustrates how Chisana lavas compare to volcanic rocks from Cenozoic continental arcs (e.g., High Cascades arc, Oregon and Wrangell Arc, Alaska). In both comparisons, Chisana rocks have similar overall patterns, including elevated LILE abundances (e.g., Rb through Sr) that likely indicate a continental lithosphere contribution (e.g., thick Wrangellia lithosphere). In comparison, Chisana lavas have dissimilar trace element patterns when compared to lavas from the East African rift (Giordano et al., 2014) as well as average OIB and N-MORB (Figure 7d). These differences do not support the hypothesis that Chisana Formation volcanism occurred due to rifting related processes. Chisana lavas partially overlap with igneous rocks from the Marianas backarc (Pearce et al., 2005). However, the Marianas rocks, while showing a subduction influence, also have much more depleted (e.g., MORB-like) LILE concentrations (Figure 7d).

Our Sr-Nd-Pb isotope results are similar to earlier published Sr-Nd-Pb data from four Chisana lavas from Bonanza Creek reported by Aleinikoff et al. (2000) (Figure 9). Chisana lavas and the ~117–113 Ma White Mountain intrusive samples yield geochemical compositions and isotope characteristics that overlap with magmas from volcanic suites formed within juvenile continental crust (e.g., Wrangell Arc) and immature island arcs (e.g., Aleutians, Marianas), suggesting that they were derived via subduction (Figures 9a and 9b) (Snyder & Hart, 2007). The Nd compositions of Chisana lavas ($\varepsilon Nd_{120} > 8$) argue against substantial interaction with (or solely melting of) ancient continental lithosphere ($\varepsilon Nd < -10$ to -30) (Mezger et al., 2001) during magmatism (Figure 7). Supporting this interpretation are Sr and Nd isotope data ($^{87}Sr/^{86}Sr_i = 0.70329–0.70423$; $\varepsilon Nd_i = +4.9$ to 6.1) from ~98 to 89 Ma intrusions associated with the Pebble deposit that intruded into the Kahiltna basin (Olson et al., 2017). Olson et al. (2017) interpret these data to reflect interaction of subduction-derived melts produced in a volcanic arc, with Kahiltna sediment. Like the Wrangell Arc (Berkelhammer et al., 2019; Brueseke et al., 2019), Chisana magmas erupted through the Insular terranes and this is reflected by Devonian to Jurassic Nd depleted-mantle model ages from the White Mountain intrusive body (Snyder & Hart, 2007), and the continental lithosphere contribution implied by Chisana LILE abundances (Figure 7).

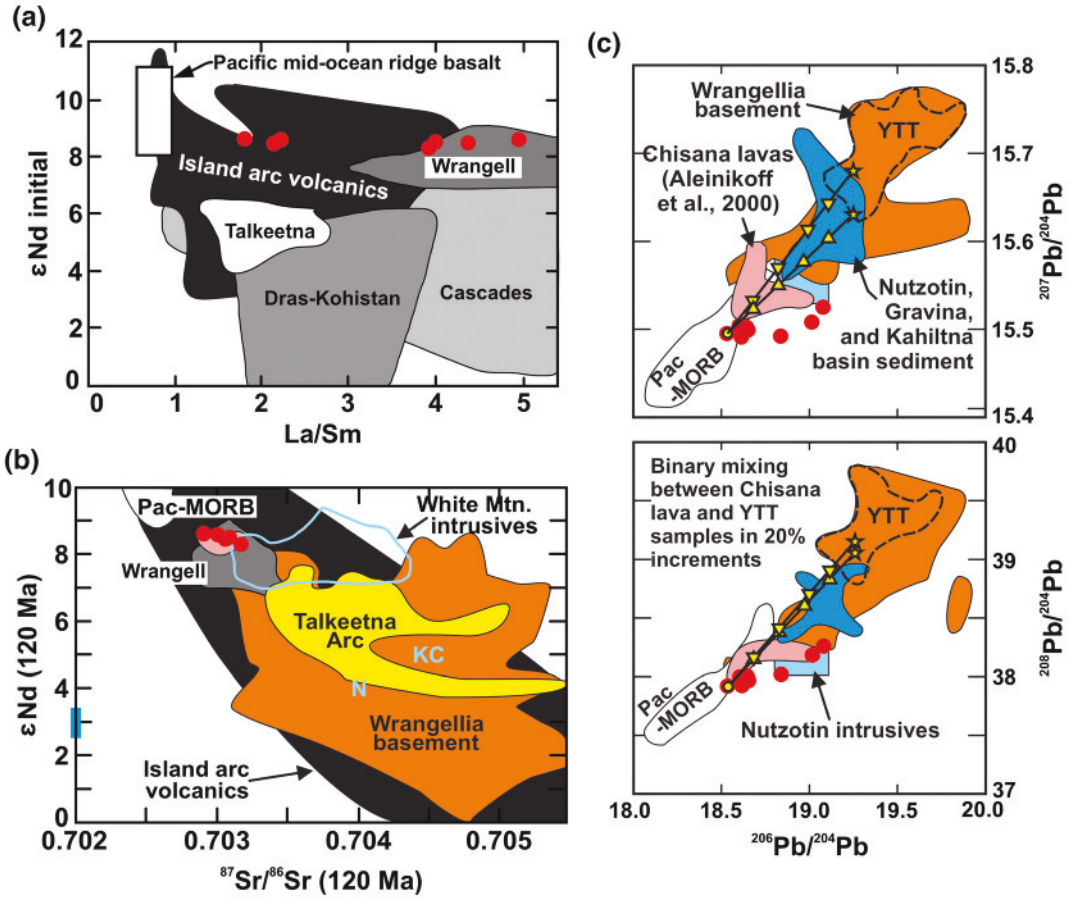


Figure 9. Trace element and isotope compositions of Chisana lavas from Bonanza Creek (Figure 3). (a) Diagram after Clift, Draut, et al. (2005) showing constant Nd isotope composition with increasing LREE enrichment within the Chisana lavas. Note overlap with modern continental (i.e., Wrangell Arc; Brueseke et al., 2019; Preece & Hart, 2004) and oceanic island arcs (e.g., Aleutians, Tonga, Marianas, Izu-Bonin). (b) Nd and Sr isotope compositions of Chisana lavas. Note overlap with magmas that erupted through the Insular terranes (<30 Ma Wrangell Arc and ~117–113 Ma White Mountain intrusives; Figure 3. Blue bar denotes epsilon Nd range of volcaniclastic rocks from the Dezadeash Basin (Figures 1 and 2; Lowey, 2011). N, ~118 Ma Nabesna pluton; KC, ~125–115 Klein Creek pluton (Figure 3) (Graham et al., 2016). (c) $^{206}Pb/^{204}Pb$ versus $^{208}Pb/^{204}Pb$ and $^{207}Pb/^{204}Pb$. Isotope data from this study overlap with Pacific MORB but extends to slightly more radiogenic ratios (e.g., toward local crust and suture zone sediments). Wrangellia basement field contains Wrangellia rocks from Canada and Alaska (Lassiter & Mahoney, 1995; Preece, 1997) and Nikolai Greenstone (Greene et al., 2008; Greene et al., 2009). Cretaceous basin sediment (Kahiltna, Gravina, Nutzotin basin) and other Chisana Formation lavas from Aleinikoff et al. (2000). YTT, Yukon-Tanana rocks and feldspars (Aleinikoff et al., 2000). Mixing between Chisana basalt lava (CH1-1395) and two representative YTT granitoids in 20% increments. Nutzotin intrusives = Pb isotope ratios range from Nabesna and Klein Creek plutons reported by Graham et al. (2016).

Our new data also have similar Pb isotope ratios to those reported by Graham et al. (2016) for two other Nutzotin basin intrusives, the ~118 Ma Nabesna pluton and ~125–115 Klein Creek pluton (Figure 3). Other radiogenic isotope data from Insular terrane basement in proximity to our study areas is limited (e.g., Greene et al., 2008, 2009; Lassiter & Mahoney, 1995; Preece, 1997), however, Figures 9b and 9c show that Chisana lavas have different Sr-Nd-Pb isotope characteristics than Insular terrane basement rocks. Furthermore, the isotope data we report here also has different Nd and Pb isotope ratios than Nutzotin-Gravina-Kahiltna basin sediment (Figures 9b and 9c). Chisana lavas are also isotopically dissimilar to ancient North American lithosphere (e.g., Yukon-Tanana Terrane; YTT, Figure 9c). Simple mixing curves between a Chisana basalt and two isotopically distinct, but representative, YTT granitoids illustrate that Chisana Pb isotope compositions were not likely influenced by a substantial (if any) YTT component and is consistent with Nd isotope data discussed above. This observation has important implications for the inferred position of the Chisana arc relative to the continental margin during Early Cretaceous Chisana magmatism and the polarity of the Chisana arc subduction zone; we expand on this below. The Pb isotope compositions of Chisana lavas do plot close to those reported from Cretaceous sedimentary strata within the

suture zone sediments and local crust (e.g., Nutzotin intrusives and Insular terrane basement), again consistent with some interaction with Insular terrane lithosphere. Further isotope characterization of the pre-Chisana igneous rocks of the Insular terranes is needed to fully address the mantle and crustal inputs that affected Chisana lavas.

5.3. Origin of the Chisana Formation and Tectonic Implications

The tectonic cause of Jurassic-Cretaceous volcanic and sedimentary strata along the inboard margin of the Insular terranes (i.e., the Gravina-Nutzotin belt) is a debated subject (Lowey, 2017; Yokelson et al., 2015). Studies from southeastern Alaska and British Columbia suggest that the Insular terranes had collided with inboard terranes by Middle Jurassic time (Gehrels, 2001; McClelland & Gehrels, 1990). There, Late Jurassic-Early Cretaceous volcanism and sedimentation occurred in postcollisional, backarc basins that were closed during mid-Cretaceous shortening (Armstrong, 1988; van Der Heyden, 1992) or transtensional basins that were created by strike-slip fault systems (Figure 10d) (Gehrels et al., 2009; McClelland et al., 1992). Studies from south central Alaska and Yukon Territory propose that volcanism is related to east dipping subduction and that basin development evolved from an offshore Jurassic intra-oceanic arc to a late Early to Late Cretaceous collisional arc setting (Figure 10c) (Goddard et al., 2018; Hampton et al., 2010; Trop et al., 2020; Trop & Ridgway, 2007). Other models suggest that magmatism reflects east dipping intra-oceanic subduction beneath the Insular terranes prior to Late Cretaceous collision with inboard terranes (Figure 10a) (Berg et al., 1972; Monger et al., 1982; Nokleberg et al., 1985) or west dipping intra-oceanic subduction beneath the Insular terranes prior to collision with inboard terranes (Figure 10b; Lowey, 2017; Sigloch & Mihalynuk, 2013; Sigloch, 2017).

Sedimentary facies similar to the volcaniclastic conglomerate facies we identified are found in modern arcs, such as the Mariana or Tonga arcs and are interpreted as primary volcanic and mass wasting deposits proximal to an active arc volcano (Draut & Clift, 2006). The similarities of the sedimentary facies of the Chisana Formation and the sedimentary facies found in the Talkeetna, Mariana and Tonga arcs lend further credence to the hypothesis that the Chisana Formation was part of an island-arc system. Lithofacies of the lower and middle sections of the Chisana Formation at Bonanza Creek are very similar to lithofacies associations of the Talkeetna Formation at Sheep Mountain, or debris aprons formed around volcanic centers of the Tonga arc (Draut & Clift, 2006). Abundance of volcaniclastic turbidite facies, along with the presence of lahar breccias and block and ash deposits in the middle section of the Chisana Formation at Bonanza Creek, all suggest that deposition occurred <10 km from the volcanic vent (Draut & Clift, 2006). Lithofacies from the Chisana Formation are also consistent with lithofacies of "fringing" island arcs, such as the Cretaceous Alisitos arc reported by Busby (2004) and Busby et al. (2006). Furthermore, thick successions of siliciclastic strata occur south of the Chisana Formation in the Wrangell Mountains basin and are interpreted to have been deposited in a forearc basin positioned outboard of the Chisana arc (Plafker & Berg, 1994; Trop et al., 2002). The Chisana arc was a major sediment source to this basin during late Early to early Late Cretaceous time judging from compositional and detrital geochronological data (Trop et al., 2002; Fasulo, 2019; Fasulo et al., 2020). The presence of these forearc deposits, together with coeval subduction complex deposits to the south in the Chugach terrane (Amato et al., 2013), are consistent with models that attribute Chisana magmatism to island arc-formation above an east dipping subduction zone (Figures 10a and 10c–10e). If a west dipping subduction zone was present under the Insular terranes, one might also expect an isotope signature of subducted continental material (e.g., Yukon Tanana terrane sediment) to be present in the Chisana lavas like what has been documented for other arc-continent collisions (Draut & Clift, 2001; Elberg et al., 2002). Detrital zircon studies demonstrate that Precambrian-Paleozoic detritus eroded from the continental margin (e.g., Yukon Tanana terrane) was shed into the Kahiltna basin during late Early Cretaceous time (Hampton et al., 2010; Romero et al., 2020). However, a continental margin signature is seemingly not evident in the isotope characteristics of Chisana lavas. This is most consistent with the presence of an east dipping subduction zone under the Insular terranes, causing mantle wedge melting and arc volcanism, while the Insular terranes "backed into" the continent by the pull of second east dipping subducting slab under the inboard terranes (Figures 10a and 10c). Transtensional or rifting-related volcanism, in tectonic settings unrelated to intra-arc rifting, is usually much smaller volume relative to belts of arc volcanoes (Tibaldi et al., 2010).

The arc-affinity signatures present in the geochemistry of the Chisana Formation, regional radiogenic isotope data, combined with marine depositional environments for lavas and interbedded sediments in the

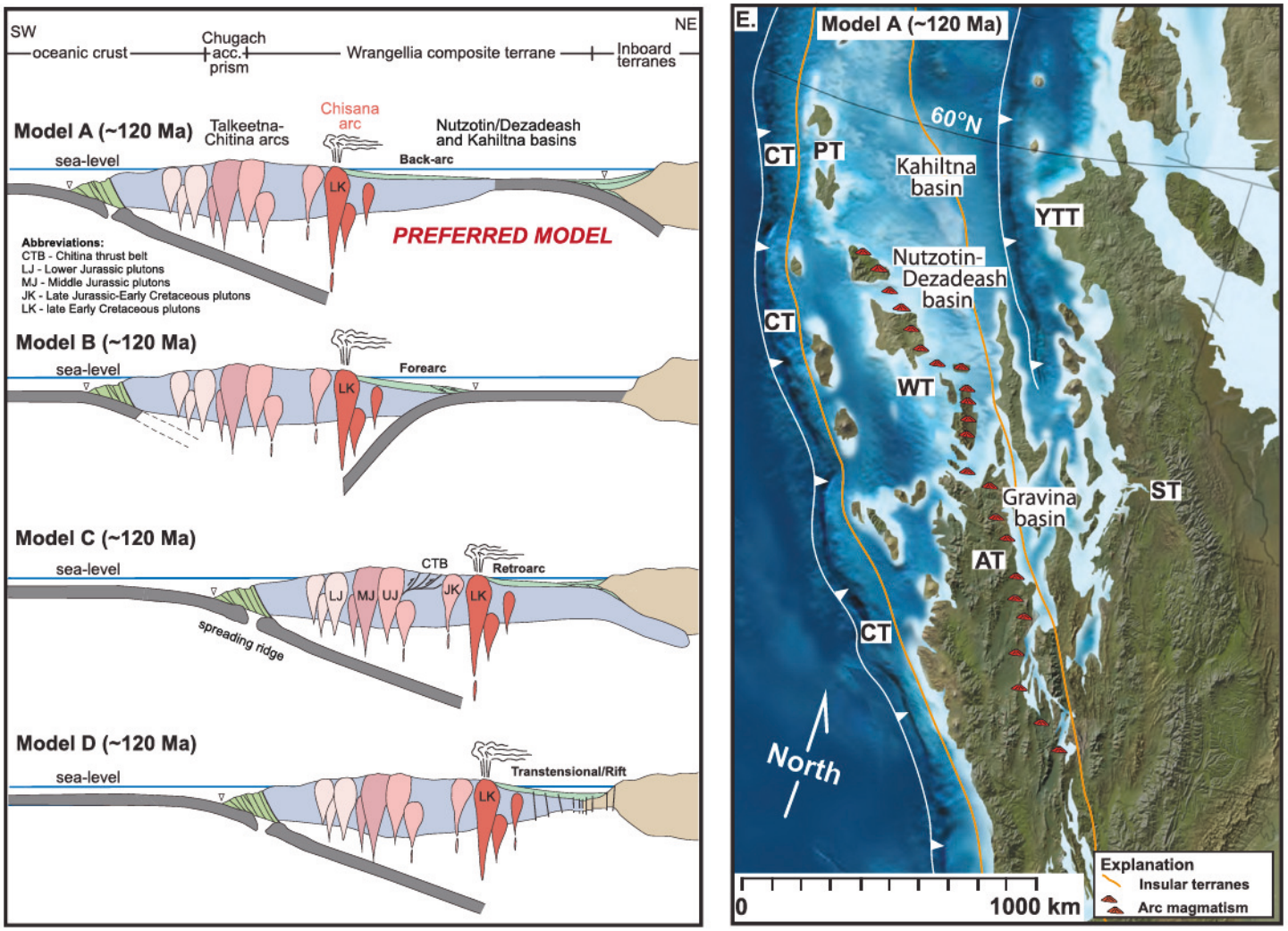


Figure 10. Previously proposed tectonic scenarios for the Insular terranes (IT) and Chisana arc magmatism during Early Cretaceous time (~120 Ma). (a) Precollisional ocean basin scenario with east dipping subduction beneath the IT, east dipping subduction beneath inboard terranes, and an ocean of indeterminate width separating the IT from inboard terranes (modified from Berg et al., 1972; Lowey, 2018). (b) Precollisional, forearc basin scenario, with west dipping subduction beneath the IT, possible east dipping subduction beneath IT (dashed lines), and a wide ocean separating the IT from inboard terranes (modified from Sigloch, 2017). (c) Syncollisional, retroarc foreland basin scenario with east dipping subduction beneath the IT, shortening along the Chitina thrust belt (CTB), and east dipping subduction beneath inboard terranes (modified from Manuszak et al., 2007; Trop et al., 2002; Trop & Ridgway, 2007). (d) Postcollisional rift or transtensional basin scenario with east dipping subduction beneath the IT and a narrow ocean separating the IT from inboard terranes (modified from McClelland et al., 1992). (e) Paleogeographic map showing our preferred tectonic model of the northwestern Cordillera ca. 120 Ma with diachronous south-to-north closure of east dipping subduction zone along the inboard (northeastern eastern) margin of the Insular terranes. In this model, northern portions of the Insular terranes presently exposed in south central and eastern Alaska changed from the model depicted in (a) to the model depicted in (c) during Late Jurassic to Late Cretaceous time consistent with the evolution of the Nutzotin and Kahiltna basins (e.g., Manuszak et al., 2007; Romero et al., 2020; Trop et al., 2019, 2020). Our preferred model for Chisana magmatism is depicted in (a); our data do not support the model in (b). Terrane abbreviations: AT = Alexander, CT = Chugach, PT = Peninsular, ST = Stikine, WT = Wrangellia, YTT = Yukon-Tanana. Chisana arc, the focus of this study, was emplaced ~130–115 Ma along the inboard (northeastern) margin of the Wrangellia and Alexander terranes. Extent of volcanism and Insular terranes is schematic.
© 2013 Colorado Plateau Geosystems Inc.

lower part of the stratigraphy, and the presence of lithofacies observed in the Chisana Formation and modern island arcs (Draut & Clift, 2006), all indicate that the Chisana Formation is the product of an island arc. Chisana Formation igneous rocks help define a ~2,000 km-long zone of magmatism (Plafker & Berg, 1994), which is inconsistent with the more localized extent of magmatism expected from transtensional tectonics alone. Additionally, basalts produced in a transtensional tectonic regime are commonly highly potassic, alkalic to transitional-tholeiitic, and usually less hydrous than what is seen in Chisana Formation lavas and plutons (e.g., hydrous mineral-bearing) (Beccaluva et al., 1998; Putirka,

2007; Tibaldi et al., 2010; Vaughan & Scarrow, 2003). Overall, the long linear array of coeval igneous rocks from south central Alaska to southeastern Alaska and coastal British Columbia are inconsistent with a model where Chisana Formation igneous rocks formed in a transtensional tectonic setting in the absence of subduction/arc magmatism. Instead, our interpretations are consistent with the tectonic model for southeastern Alaska and coastal British Columbia proposed by Gehrels et al. (2009) in which oblique plate convergence prompted regional subduction-related arc magmatism along with backarc sedimentation/volcanism. We infer that volcanic and sedimentary strata of the Chisana Formation and Nutzotin Mountains sequence accumulated along the inboard (north) flank of the west facing, extensional island arc (Figure 10). The interbedded successions of marine volcanic and sedimentary strata in the Gravina Sequence in southeastern Alaska (Berg et al., 1972; Rubin & Saleeby, 1991), differ from what we document in the Nutzotin basin. Rubin and Saleeby (1991) interpret the Gravina Sequence to represent subaqueous arc volcanism and associated sedimentation that changes upsection from a proximal to distal arc setting. However, the Gravina metabasalts have also been interpreted as rift-related (Ford and Brew, 1987), thus it is possible that Gravina Sequence may actually represent a backarc setting, relative to the active Chisana arc (e.g., Gehrels et al., 2009). Lastly, we acknowledge the possibility of large magnitudes of strike-slip displacement since early Cretaceous arc magmatism. Stratigraphic data indicate the Dezadeash and Nutzotin basins were once connected prior to ~370 km of dextral offset along the Denali fault (Figure 1; Lowey, 1998). Moreover, the basins may have formed far south of their current positions given paleomagnetic constraints from Late Cretaceous tuffs that overlie Wrangellia in the study area (e.g., Stamatakos et al., 2001).

Our results also support the model of Plafker and Berg (1994) that Late Jurassic–Early Cretaceous volcanism in the Gravina and Nutzotin basins were part of a single magmatic arc (Figure 10e). This elongate arc is referred to as the Chisana arc in eastern Alaska, the Gravina arc in southeastern Alaska, or the Gravina-Nutzotin belt. Furthermore, the mineralogy and chemical composition of Chisana lavas at Bonanza Creek (e.g., packages of amphibole bearing, calc-alkaline lavas in the lower section versus olivine-bearing, more tholeiitic compositions upsection, Figure 5) suggests that intra-arc rifting may have affected the Chisana arc (Manselle, 2019) or alternatively, the tholeiites may have been produced by a different parental melt and subsequent differentiation (Firth et al., 2019). When taken in context with other studies from southern Alaska, the results of this study provide robust evidence for east dipping subduction under the Insular terranes (Figures 10a and 10c) (Pavlis et al., 2019) rather than the alternatively proposed, west dipping subduction model (Figure 10b) (Sigloch, 2017). Studies from the Chugach terrane to the west of the study area (Amato et al., 2013; Plafker & Berg, 1994) firmly indicate that the Chugach terrane represents the remains of Late Jurassic–Early Cretaceous subduction complex. Moreover, Middle Jurassic to Early Cretaceous siliciclastic strata crop out in a forearc position between the Chugach Terrane subduction complex to the south and Middle Jurassic to Early Cretaceous volcanic-plutonic arc complexes to the north (Clift, Pavlis, et al., 2005; Clift, Draut, et al., 2005; Plafker & Berg, 1994; Talkeetna and Chisana arcs; Trop & Ridgway, 2007). Sedimentological and detrital geochronological data sets from these forearc sedimentary strata reflect erosion of Jurassic volcanic-plutonic arc source terranes and trenchward (southward) sediment transport (Goddard et al., 2018; Reid et al., 2018; Trop et al., 2005). Late Jurassic to Early Cretaceous strata that crop out in a retroarc position north of the Jurassic-Cretaceous Chisana-Chitina-Talkeetna volcanic arcs record sediment flux away from the magmatic arcs as well as sediment input from inboard terranes (e.g., Fasulo, 2019; Hampton et al., 2010; Romero et al., 2020). An inboard (northeastward relative to modern locations) shift in arc magmatism from the Jurassic Chitina arc to Cretaceous Chisana arc represents long-lived subduction under the Insular terranes (Figure 10), analogous to the inboard shift in magmatism well documented within the Insular terranes in southeastern Alaska and coastal British Columbia (i.e., Coast Ranges batholith) (Gehrels et al., 2009). The inboard magmatic shift may reflect slab shallowing due to subduction of younger crust, in response to an approaching spreading ridge that was subsequently subducted, as recorded in the upper plate by ca. 123 Ma near-trench tonalite-trondhjemite magmatism in the accretionary prism and an ~130–115 Ma unconformity in forearc basinal strata south of the study area (Barnett et al., 1994; Mahar et al., 2019; Pavlis et al., 1988; Trop & Ridgway, 2007). Collectively, our new data sets from the Chisana Formation of eastern Alaska, when combined with these other studies, support a model where formation of the Insular terranes and adjacent basins were shaped by subduction-related island arc volcanism resulting from east dipping subduction of oceanic lithosphere beneath the Insular terranes (Figures 10a and 10c).

Our new stratigraphic data from the Chisana Formation, together with recently reported data sets from the study area document subaerial uplift and deformation of the island arc and adjacent marine basins beginning in late Early Cretaceous time (Trop et al., 2020). The results of the present study demonstrate that the Chisana Formation records a distinct shift from marine to terrestrial volcanism (Figure 5). Moreover, sedimentological data and dinosaur footprints from the overlying ca. 117 to 93 Ma Beaver Lake formation (Fiorillo et al., 2012) document terrestrial conditions and connections with both the Insular terranes and inboard terranes along the former continental margin (Trop et al., 2020). The shift from relatively deep-marine submarine slope/fan environments to terrestrial deposition may have been partly related to short-term sea level regressions, however relatively high and stable sea levels characterized late Aptian–Albian time (Haq, 2014). Subaerial emergence of the formerly marine basins overlapped with regional compression within and outboard of the suture zone. Outboard of the suture zone in the Wrangell Mountains, Upper Jurassic and older sedimentary strata were deformed by regional compression prior to deposition of Albian and younger sedimentary strata along an angular unconformity (Trop et al., 2002). Within the suture zone, Jurassic–Early Cretaceous marine strata of the Nutzotin Mountains sequence were thrust onto older rocks of Wrangellia along a northeast dipping décollement prior to emplacement of an undeformed ~117 Ma pluton (Manuszak et al., 2007; Richter et al., 1975). Thus, the formerly marine Nutzotin basin evolved into a broad zone of crustal thickening through the addition of mid-Cretaceous intrusions and mid-Cretaceous deformation along regional faults. These observations are consistent with closure of the formerly marine ocean basin that separated the Insular terrane from inboard terranes. We attribute these processes to accretion/suturing of the Chisana island arc and underlying Wrangellia with the former continental margin (Figure 10e).

Our results align with data from Olson et al. (2017) who demonstrate that the ~90 Ma Kaskanak batholith, associated with the world-class Pebble Cu-Au-Mo porphyry deposit, also formed in a volcanic arc within the suture zone. The younger age of the Kaskanak batholith and associated porphyry mineralization, is consistent with tectonic models where the closure of the Gravina-Nutzotin-Kahlitna belt occurred asynchronously (Figure 10e) and porphyry mineralization and perhaps Andean-style arc magmatism (or postcollisional magmatism; Goldfarb et al., 2013) occurred in some locations along the suture zone. ~120 Ma Chisana island arc volcanism and local porphyry mineralization (e.g., Nabesna, Orange Hill, Bond Creek, etc.) and subsequent ~117–93 Ma accretion of the Chisana arc to North America (Trop et al., 2020) preceded ~101–88 Ma magmatism in the southwest Alaska Range associated with the Pebble deposit, in the same magmatic-accretionary event.

Late Cretaceous–Cenozoic plate convergence and dextral transpression along strike-slip faults prompted shortening and lateral shuffling of the Chisana arc and associated Jurassic–Cretaceous basins (Kahiltna, Nutzotin, Dezadeash, and Gravina basins) (e.g., Benowitz et al., 2011; Gehrels et al., 2009; Waldien et al., 2018). In eastern Alaska and Yukon, this deformation included ~370 km of dextral strike slip along the Denali fault that displaced previously linked marine basin deposits of the Nutzotin and Dezadeash basins (Figure 1; Lowey, 1998), and several tens of kilometers of dextral slip along the Totschunda and Duke River faults, which displaced the outboard (southern) margin of the Nutzotin basin, including Chisana arc volcanics and associated intrusions (Brueseke et al., 2019; Cobett et al., 2014; Trop et al., 2020).

6. Conclusions

The Chisana Formation is a >2 km thick succession of late Early Cretaceous volcanic, volcaniclastic, and minor sedimentary strata that crop out extensively in the Nutzotin Mountains of eastern Alaska (Figure 2). Whole rock geochemical and Sr-Nd-Pb isotope data and lithofacies strongly support an island arc origin for the Chisana Formation. However, stratigraphic and geochemical data sets from underlying successions (Greene et al., 2008, 2009) suggest that Chisana Formation magmas erupted through significantly thickened crust as opposed to “typical” oceanic crust. Geochemical data presented here can be used to verify earlier inferences that the Chisana Formation is part of a long-lived Chisana arc (Plafker & Berg, 1994) and correlate to Gravina belt metavolcanic rocks exposed along the inboard margin of the Alexander terrane in southeastern Alaska (McClelland et al., 1992; Rubin & Saleeby, 1991; Stowell et al., 2000).

Geochemical similarities between Cretaceous-aged plutons in the Nutzotin Mountains and Chisana Formation igneous rocks are consistent with the hypothesis that these Cretaceous intrusives also represent magmatism in part of the Chisana arc. Data from this study, combined with (1) subduction complex deposits coeval with the Chisana Formation in the Chugach Mountains (Plafker & Berg, 1994); and (2) Chisana Formation-aged basinal strata located in a forearc position relative to the Chisana arc (Goddard et al., 2018; Reid et al., 2018; Trop et al., 2002) and a backarc/retroarc position to the north in the Nutzotin and Kahiltna basins (Box et al., 2019; Fasulo, 2019; Hampton et al., 2010; Hults et al., 2013; Kalbas et al., 2007; Manuszak et al., 2007) reflect an island arc origin associated with an east dipping subduction zone beneath the Insular terranes. An upsection shift from marine to terrestrial depositional conditions documented in the Chisana Formation and the overlying ~117–93 Ma Beaver Lake formation was coincident with regional shortening. Together, the geologic evidence for shortening and terrestrial deposition are interpreted to reflect accretion of the Chisana island arc and Wrangellia against inboard terranes. Postaccretionary dextral slip along the Denali-Totschunda-Duke River strike-slip faults has displaced much of the Chisana arc and associated marine basins.

Data Availability Statement

All supporting analytical data and figures can be found online as supporting information and also are available online (at the following link: 10.6084/m9.figshare.11837016).

Acknowledgments

This research was part of Manselle's MS thesis at Kansas State. It was made possible in part by funding from NSF to Brueseke (EAR-1450689), Benowitz (EAR-1450730), and Trop (EAR-1450687). We thank everyone at Devil's Mountain Lodge for field/air support, NPS personnel at Wrangell-St. Elias National Park and Preserve for assistance, Paul O'Sullivan for geochronological analyses, and Garth Graham for sharing geochronologic data and sample locations. We are indebted to Ken Ridgway for thoughtful discussion and assistance collecting pilot samples along Bonanza Creek and to Emily Heuer (Short) for contributions to geochemical analyses of pilot samples along Bonanza Creek as an undergraduate project. We also thank reviewers Cathy Busby and Luke Beranek for their constructive feedback and Margaret Rusmore for handling this manuscript.

References

Aleinikoff, J. N., Farmer, G. L., Rye, R. O., & Nokleberg, W. J. (2000). Isotopic evidence for the sources of Cretaceous and Tertiary granitic rocks, east-central Alaska: Implications for the tectonic evolution of the Yukon-Tanana Terrane. *Canadian Journal of Earth Sciences*, *37*(6), 945–956. https://doi.org/10.1139/e00-006

Allam, A., Schulte-Pelkum, V., Ben-Zion, Y., Tape, C., Ruppert, N., & Ross, Z. (2017). Ten kilometer vertical Moho offset and shallow velocity contrast along the Denali fault zone from double-difference tomography, receiver functions, and fault zone head waves. *Tectonophysics*, *721*, 56–69. https://doi.org/10.1016/j.tecto.2017.09.003

Amato, J. M., Pavlis, T. L., Clift, P. D., Kochelek, E. J., Hecker, J. P., Worthman, C. M., & Day, E. M. (2013). Architecture of the Chugach accretionary complex as revealed by detrital zircon ages and lithologic variations: Evidence for Mesozoic subduction erosion in south-central Alaska. *Geological Society of America Bulletin*, *125*(11-12), 1891–1911. https://doi.org/10.1130/b30818.1

Armstrong, R. L. (1988). Mesozoic and early Cenozoic magmatic evolution of the Canadian Cordillera. *Geological Society of America Special Papers*, *218*, 55–91.

Barker, F., Aleinikoff, J. N., Box, S. E., Evans, B. W., Gehrels, G. E., Hill, M. D., et al. (1994). Some accreted volcanic rocks of Alaska and their elemental abundances. In G. Plafker, H. C. Berg, & Geological Society of America, The Geology of North America, v. G-1 (Eds.), *The geology of Alaska*. (pp. 555–587). Colorado: Boulder

Barnett, D. E., Bowman, J. R., Pavlis, T. L., Rubenstone, J. R., Snee, L. W., & Onstott, T. C. (1994). Metamorphism and near-trench plutonism during initial accretion of the Cretaceous Alaskan forearc. *Journal of Geophysical Research: Solid Earth*, *99*(B12), 24,007–24,024. https://doi.org/10.1029/94JB02462

Beccaluva, L., Siena, F., Coltorti, M., Di Grande, A., Lo Giuduce, A., Macciotta, G., et al. (1998). Nephelinitic to tholeiitic magma generation in a transtensional tectonic setting: An integrated model for the Iblean volcanism, Sicily. *Journal of Petroleum*, *39*, 1547–1576

Benowitz, J. A., Layer, P. W., Armstrong, P., Perry, S. E., Haeussler, P. J., Fitzgerald, P. G., & VanLaningham, S. (2011). Spatial variations in focused exhumation along a continental-scale strike-slip fault: The Denali fault of the eastern Alaska Range. *Geosphere*, *7*(2), 455–467. https://doi.org/10.1130/ges00589.1

Beranek, L. P., McClelland, W. C., van Staal, C. R., Israel, S., & Gordee, S. M. (2017). Late Jurassic flare-up of the Coast Mountains arc system. *NW Canada, and dynamic linkages across the northern Cordilleran orogen, Tectonics*, *36*, 877–901. https://doi.org/10.1002/2016TC004254

Beranek, L. P., & Mortensen, J. K. (2011). The timing and provenance record of the Late Permian Klondike orogeny in northwestern Canada and arc-continent collision along western North America. *Tectonics*, *30*(5). https://doi.org/10.1029/2010tc002849

Berg, H. C., Jones, D. L., & Richter, D. H. (1972). Gravina-Nutzotin belt; tectonic significance of an upper Mesozoic sedimentary and volcanic sequence in southern and southeastern Alaska, *U.S. Geological Survey Professional Paper*, *800-D*, D1–D24

Berkelhammer, S. E., Brueseke, M. E., Benowitz, J. A., Trop, J. M., Davis, K., Layer, P. W., & Weber, M. (2019). Geochemical and geochronological records of tectonic changes along a flat-slab arc-transform junction: Circa 30 Ma to ca. 19 Ma Sonya Creek volcanic field, Wrangell Arc, Alaska. *Geosphere*, *15*(5), 1508–1538

Beswick, A., & Soucie, G. (1978). A correction procedure for metasomatism in an Archean greenstone belt. *Precambrian Research*, *6*(2), 235–248. https://doi.org/10.1016/0301-9268(78)90015-3

Box, S. E., Karl, S. M., Jones, J. V. III, Bradley, D. C., Haeussler, P. J., & O'Sullivan, P. B. (2019). Detrital zircon geochronology along a structural transect across the Kahiltna assemblage in the western Alaska Range: Implications for emplacement of the Alexander-Wrangellia-Peninsular terrane against North America. *Geosphere*, *15*(6), 1774–1808. https://doi.org/10.1130/GES02060.1

Brennan, P. R. K., Gilbert, H., & Ridgway, K. D. (2011). Crustal structure across the central Alaska Range: Anatomy of a Mesozoic collisional zone. *Geochemistry, Geophysics, Geosystems*, *12*, Q04010. https://doi.org/10.1029/2011gc003519

Brueseke, M. E., Benowitz, J. A., Trop, J. M., Davis, K. N., Berkelhammer, S. E., Layer, P. W., & Morter, B. K. (2019). The Alaska Wrangell Arc: ~30 million years of subduction-related magmatism along a still active arc-transform junction. *Terra Nova*, *31*, 59, ter.12369–66. https://doi.org/10.1111/ter.12369

Busby, C. (2004). Continental growth at convergent margins facing large ocean basins: A case study from Mesozoic convergent-margin basins of Baja California. *Mexico, Tectonophysics*, *392*(1-4), 241–277. https://doi.org/10.1016/j.tecto.2004.04.017

Busby, C. J., Fackler Adams, B., Mattinson, J., & De Oreo, S. (2006). View of an intact oceanic arc, from surficial to mesozonal levels: Cretaceous Alisitos Arc, Baja California, Mexico. *Journal of Volcanology and Geothermal Research*, *149*(1-2), 1–46

Cecil, M. R., Gehrels, G., Ducea, M. N., & Patchett, P. J. (2011). U-Pb-Hf characterization of the central Coast Mountains batholith: Implications for petrogenesis and crustal architecture. *Lithosphere*, *3*(4), 247–260. https://doi.org/10.1130/l134.1

Cecil, M. R., Rusmore, M. E., Gehrels, G. E., Woodsworth, G. J., Stowell, H. H., Yokelson, I. N., et al. (2018). Along-strike variation in the magmatic tempo of the Coast Mountains batholith, British Columbia, and implications for processes controlling episodicity in arcs. *Geochemistry, Geophysics, Geosystems*, *19*, 4274–4289. https://doi.org/10.1029/2018gc007874

Clift, P. D., Pavlis, T., DeBari, S. M., Draut, A. E., Rioux, M., & Kelemen, P. B. (2005). Subduction erosion of the Jurassic Talkeetna-Bonanza arc and the Mesozoic accretionary tectonics of western North America. *Geology*, *33*(11), 881–884. https://doi.org/10.1130/g21822.1

Clift, P. D., Draut, A. E., Kelemen, P. B., Blusztajn, J., & Greene, A. (2005). Stratigraphic and geochemical evolution of an oceanic arc upper crustal section: The Jurassic Talkeetna volcanic formation, south-central Alaska. *Geological Society of America Bulletin*, *117*(7), 902–925. https://doi.org/10.1130/B25638.1

Colpron, M., Nelson, J. L., & Murphy, D. C. (2007). Northern Cordilleran terranes and their interactions through time. *GSA Today*, *17*(4), 4. https://doi.org/10.1130/gsat01704-5a.1

Compton, R. R. (1985). Geology in the field: Cape Town, Earthspun Books

Coney, P. J., Jones, D. L., & Monger, J. W. H. (1980). Cordilleran suspect terranes. *Nature*, *288*(5789), 329–333. https://doi.org/10.1038/288329a0

Crawford, M. L., Hollister, L. S., & Woodsworth, G. J. (1987). Crustal deformation and regional metamorphism across a terrane boundary, Coast Plutonic Complex, British Columbia. *Tectonics*, *6*(3), 343–361. https://doi.org/10.1029/tc006i003p00343

Csejtey Jr. B., Mullen, M. W., Cox, D. P., & Stricker, G. D. (1992). Geology and geochronology of the Healy quadrangle, south-central Alaska, *U.S. Geological Survey Misc. Invest. Series Map I-1961,* 1:250,000 scale

DeBari, S., Heywood, L. & Gill, J. (2020). Izu Bonin Across arc geochemical dataset between latitudes 32°40′ to 30°20′, *v.1.0*. Interdisciplinary Earth Data Alliance (IEDA). https://doi.org/10.1594/IEDA/111493. Accessed 2020-04-08

Draut, A. E., & Clift, P. D. (2001). Geochemical evolution of arc magmatism during arc-continent collision, South Mayo, Ireland. *Geology*, *29*, 543–546

Draut, A. E., & Clift, P. D. (2006). Sedimentary processes in modern and ancient oceanic arc settings: Evidence from the Jurassic Talkeetna formation of Alaska and the Mariana and Tonga arcs, western Pacific. *Journal of Sedimentary Research*, *76*(3), 493–514. https://doi.org/10.2110/jsr.2006.044

Ducea, M. N., Saleeby, J. B., & Bergantz, G. (2015). The architecture, chemistry, and evolution of continental magmatic arcs. *Annual Review of Earth and Planetary Sciences*, *43*(1), 299–331. https://doi.org/10.1146/annurev-earth-060614-105049

Fasulo, C. R. (2019). Sedimentary record of tectonic growth along a convergent margin: Insights from detrital zircon geochronology of Mesozoic sedimentary basins and modern rivers in south-central Alaska (Doctoral dissertation, Purdue University Graduate School)

Fasulo, C. R., Ridgway, K. D., Allen, W. K., Romero, M. C., & Keough, B. (2018). U-Pb and Hf isotope detrital zircon geochronology of the Nutzotin Mountains sequence, south-central Alaska: Implications for the configuration of the Mesozoic convergent margin, NW Cordillera: *Geological Society of America Abstracts with Programs, 50*, Paper 46–7, https://doi.org/10.1130/abs/2018AM-322455

Fasulo, C. R., Ridgway, K. D., & Trop, J. M. (2020). Detrital zircon geochronology and Hf isotope geochemistry of Mesozoic sedimentary basins in south-central Alaska: Insights into regional sediment transport, basin development, and tectonics along the NW Cordilleran margin. *Geosphere*. https://doi.org/10.1130/ges02221.1

Finzel, E. S., Trop, J. M., Ridgway, K. D., & Enkelmann, E. (2011). Upper plate proxies for flat-slab subduction processes in southern Alaska. *Earth and Planetary Science Letters*, *303*(3-4), 348–360. https://doi.org/10.1016/j.epsl.2011.01.014

Fiorillo, A. R., & Adams, T. L. (2012). A therizinosaur track from the Lower Cantwell Formation (Upper Cretaceous) of Denali National Park, Alaska. *PALAIOS*, *27*(6), 395–400. https://doi.org/10.2110/palo.2011.p11-083r

Firth, C., Adam, J., Turmer, S., Rushmer, T., Brens, R., Green, T. H., et al. (2019). Experimental constraints on the differentiation of low-alkali magmas beneath the Tonga arc: Implications for the origin of arc tholeiites. *Lithos*, *344-345*, 440–451. https://doi.org/10.1016/j.lithos.2019.07.008

Foster, H. L., Keith, T. E. C., & Menzie, W. D. (1994). Geology of the Yukon-Tanana area of east-central Alaska. In G. Plafker, H. C. Berg, & Geological Society of America, The Geology of North America, v. G-1 (Eds.), *The geology of Alaska*. (pp. 205–240). Colorado: Boulder. https://doi.org/10.1130/dnag-gna-g1.205

Gabrielse, H., Murphy, D. C., & Mortensen, J. K. (2006). Cretaceous and Cenozoic dextral orogen-parallel displacements, magmatism, and paleogeography, north-central Canadian Cordillera, in, *Paleogeography* of the North American Cordillera: Evidence for and against large-scale displacements. In J. W. Haggart, R. J. Enkin, & J. W. H. Monger (Eds.), (Vol. *46*, pp. 255–276). Geological Association of Canada Special Paper

Gehrels, G. E. (2000). Reconnaissance geology and U-Pb geochronology of the west flank of the Coast Mountains between Juneau and Skagway, southeastern Alaska, in *Tectonics of the Coast Mountains*, southeastern Alaska and British Columbia, edited by H. F. Stowell and W. E. *McClelland, Geological Society of America Special Paper*, *343*, 213–233. https://doi.org/10.1130/0-8137-2343-4.213

Gehrels, G. E. (2001). Geology of the Chatham Sound region, southeast Alaska and coastal British Columbia. *Canadian Journal of Earth Sciences*, *38*(11), 1579–1599. https://doi.org/10.1139/e01-040

Gehrels, G. E., Mcclelland, W. C., Samson, S. D., Patchett, P. J., & Orchard, M. J. (1992). Geology of the western flank of the Coast Mountains between Cape Fanshaw and Taku Inlet, southeastern Alaska. *Tectonics*, *11*(3), 567–585. https://doi.org/10.1029/92tc00482

Gehrels, G., Rusmore, M., Woodsworth, G., Crawford, M., Andronicos, C., Hollister, L., et al. (2009). U-Th-Pb geochronology of the Coast Mountains batholith in north-coastal British Columbia: Constraints on age and tectonic evolution. *Geological Society of America Bulletin*, *121*(9-10), 1341–1361. https://doi.org/10.1130/b26404.1

Giordano, F., Dantonio, M., Civetta, L., Tonarini, S., Orsi, G., Ayalew, D., et al. (2014). Genesis and evolution of mafic and felsic magmas at Quaternary volcanoes within the Main Ethiopian Rift: Insights from Gedemsa and Fanta Ale complexes. *Lithos*, *188*, 130–144. https://doi.org/10.1016/j.lithos.2013.08.008

Goddard, A. L. S., Trop, J. M., & Ridgway, K. D. (2018). Detrital zircon record of a Mesozoic collisional forearc basin in south central Alaska: The tectonic transition from an oceanic to continental arc. *Tectonics*, *37*, 529–557. https://doi.org/10.1002/2017tc004825

Goldfarb, R. J., Anderson, E. D., & Hart, C. J. R. (2013). Tectonic setting of the Pebble and other copper-gold-molybdenum porphyry deposits within the evolving middle Cretaceous continental margin of northwestern North America. *Economic Geology*, *108*(3), 405–419. https://doi.org/10.2113/econgeo.108.3.405

Graham, G., Kelley, K., Holm-Denoma, C., Ayuso, R., Kokaly, R., Hoefen, T., & Selby, D. (2016). Geochronology and Nd-Sr-Pb isotopic compositions of early intrusions and associated porphyry Cu deposits in eastern Alaska. In *Abstract 35th International Geological Congress*, International Geological Congress.

Greene, A. R., Scoates, J. S., & Weis, D. (2008). Wrangellia flood basalts in Alaska: A record of plume-lithosphere interaction in a Late Triassic accreted oceanic plateau. *Geochemistry, Geophysics, Geosystems*, *9*, Q12004. https://doi.org/10.1029/2008GC002092

Greene, A. R., Scoates, J. S., Weis, D., & Israel, S. (2009). Geochemistry of Triassic flood basalts from the Yukon (Canada) segment of the accreted Wrangellia oceanic plateau. *Lithos*, *110*(1-4), 1–19. https://doi.org/10.1016/j.lithos.2008.11.010

Haeussler, P. J. (1992). Structural evolution of an arc-basin: The Gravina Belt in central southeastern Alaska. *Tectonics*, *11*(6), 1245–1265. https://doi.org/10.1029/92tc01107

Hampton, B. A., Jacobs, M. R., & Stopka, C. J. (2017). U-Pb detrital geochronology and Hf isotopic analyses from upper Cretaceous strata of the northern Talkeetna Mountains, southern Alaska: Sediment dispersal and magmatism during the final accretionary phase of the Wrangellia Composite Terrane, *Geol. Soc.* America Abs w/Programs, *49*, https://doi.org/10.1130/abs/2017am-308255

Hampton, B. A., Ridgway, K. D., & Gehrels, G. E. (2010). A detrital record of Mesozoic island arc accretion and exhumation in the North American Cordillera: U-Pb geochronology of the Kahiltna basin, southern Alaska. *Tectonics*, *29*, TC4015. https://doi.org/10.1029/2009tc002544

Haq, B. U. (2014). Cretaceous eustasy revisited. *Global and Planetary Change*, *113*, 44–58. https://doi.org/10.1016/j.gloplacha.2013.12.007

Hults, C. P., Wilson, F. H., Donelick, R. A., & O'Sullivan, P. B. (2013). Two flysch belts having distinctly different provenance suggest no stratigraphic link between the Wrangellia composite terrane and the paleo-Alaskan margin. *Lithosphere*, *5*(6), 575–594. https://doi.org/10.1130/L310.1

Irvine, T. N., & Baragar, W. R. A. (1971). A guide to the chemical classification of the common volcanic rocks. *Canadian Journal of Earth Sciences*, *8*, 523–548

Kalbas, J. L., Ridgway, K. D., & Gehrels, G. E. (2007). Stratigraphy, depositional systems, and provenance of the Lower Cretaceous Kahiltna assemblage, western Alaska Range: Basin development in response to oblique collision. In K. D. Ridgway J. M. Trop J. M. G. Glen & M. O'Neill (Eds.), *Tectonic growth of a collisional continental margin: Crustal evolution of southern Alaska* (Vol. 431, pp. 307). Boulder, CO: Geological Society of America Special Paper. https://doi.org/10.1130/2007.2431(13)

Kapp, P. A., & Gehrels, G. E. (1998). Detrital zircon constraints on the tectonic evolution of the Gravina belt, southeastern Alaska. *Canadian Journal of Earth Sciences*, *35*(3), 253–268. https://doi.org/10.1139/e97-110

Lassiter, J.C., DePaolo, D.J., & Mahoney, J.J. (1995). Geochemistry of the Wrangellia flood basalt province: Implications for the role on continental and oceanic lithosphere in flood basalt genesis: *Journal of Petrology*, *36*(4), 983–1009. https://doi.org/10.1093/petrology/36.4.983

Le Bas, M. J., Le Maitre, R. W., Streckeisen, A., & Zanettin, B. (1986). A chemical classification of volcanic rocks based on the total alkali-silica diagram. *Journal of Petrology*, *27*(3), 745–750. https://doi.org/10.1093/petrology/27.3.745

Le Maitre, R. W. (1976). The chemical variability of some common igneous rocks. *Journal of Petrology*, *17*(4), 589–598. https://doi.org/10.1093/petrology/17.4.589

Löwe, P. C., Richter, D. H., & Schmoll, H. R. (1982). Geologic map of the Nabesna B-5 quadrangle, Alaska, *U.S.* Geological Survey *Geol. Quad. Map, 1566*, 1 sheet, scale 1:63,360

Lowey, G. W. (1998). A new estimate of the amount of displacement on the Denali fault system based on the occurrence of carbonate megaboulders in the Dezadeash formation (Jura-Cretaceous), Yukon, and the Nutzotin Mountains sequence (Jura-Cretaceous), Alaska. *Bulletin of Canadian Petroleum Geology*, *46*(3), 379–386

Lowey, G. W. (2007). Lithofacies analysis of the Dezadeash Formation (Jura–Cretaceous), Yukon, Canada: The depositional architecture of a mud/sand-rich turbidite system. *Sedimentary Geology*, *198*(3-4), 273–291. https://doi.org/10.1016/j.sedgeo.2006.12.011

Lowey, G. W. (2011). Volcaniclastic gravity flow deposits in the Dezadeash formation (Jura-Cretaceous), Yukon, Canada: Implications regarding the tectonomagmatic evolution of the Chitina arc in the northern Cordillera of North America. *Lithos*, *125*(1-2), 86–100. https://doi.org/10.1016/j.lithos.2011.01.014

Lowey, G. W. (2017). Comment on "U-Pb and Hf isotope analysis of detrital zircons from Mesozoic strata of the Gravina belt, southeast Alaska" by Yokelson et al. (2015). *Tectonics*, *36*, 2736–2740. https://doi.org/10.1002/2017TC004507

Lowey, G. W. (2018). Provenance analysis of the Dezadeash formation (Jurassic–Cretaceous), Yukon, Canada: Implications regarding a linkage between the Wrangellia composite terrane and the western margin of Laurasia. *Canadian Journal of Earth Sciences*, *56*(1), 77–100. https://doi.org/10.1139/cjes-2017-0244

Mahar, M. A., Pavlis, T. L., Bowman, J. R., Conrad, W. K., & Goodell, P. C. (2019). Early Cretaceous ridge subduction beneath southern Alaska: Insights from zircon U-Pb geochronology, hafnium, and oxygen isotopic compositions of the Western Chugach tonalite-trondhjemite suite. *Geological Society of America Bulletin*, *131*(3-4), 521–546. https://doi.org/10.1130/B31918.1

Manselle, P. M. (2019). Physical volcanology, sedimentology and geochemistry of the mid-Cretaceous Chisana Formation, south-central Alaska: Implications for models of Wrangellia composite terrane accretion (MS thesis). Retrieved from K-Rex. (https://krex.k-state.edu/dspace/handle/2097/39752). Manhattan, KS: Kansas State University

Manuszak, J. D., Ridgway, K. D., Trop, J. M., & Gehrels, G. E. (2007). Sedimentary record of the tectonic growth of a collisional continental margin: Upper Jurassic–Lower Cretaceous Nutzotin Mountains sequence, eastern Alaska Range, Alaska. In K. D. Ridgway, J. M. Trop, J. M. G. Glen, & M. O'Neill (Eds.), *Tectonic growth of a collisional continental margin: Crustal evolution of southern Alaska*. (Vol. 431, pp. 345–377). Boulder, CO: Geological Society of America Special Paper. https://doi.org/10.1130/2007.2431(14)

McClelland, W. C., & Gehrels, G. E. (1990). Geology of the Duncan canal shear zone: Evidence for early to middle Jurassic deformation of the Alexander terrane, southeastern Alaska. *Geological Society of America Bulletin*, *102*(10), 1378–1392. https://doi.org/10.1130/0016-7606(1990)102<1378:gotdcs>2.3.co;2

McClelland, W. C., Gehrels, G. E., & Saleeby, J. B. (1992). Upper Jurassic-Lower Cretaceous basinal strata along the Cordilleran margin: Implications for the accretionary history of the Alexander-Wrangellia-Peninsular terrane. *Tectonics*, *11*(4), 823–835. https://doi.org/10.1029/92tc00241

Mezger, J. E., Creaser, R. A., Erdmer, P., & Johnston, S. T. (2001). A Cretaceous back-arc basin in the Coast Belt of the northern Canadian Cordillera: Evidence from geochemical and neodymium isotope characteristics of the Kluane metamorphic assemblage, southwest Yukon. *Canadian Journal of Earth Sciences*, *38*(1), 91–103. https://doi.org/10.1139/e00-076

Moll-Stalcup, E. J. (1994). Latest Cretaceous and Cenozoic magmatism in mainland Alaska. In G. Plafker, & H. C. Berg (Eds.), *The geology of Alaska, Geological Society of America, The Geology of North America, v.G-1* (pp. 589–619). Boulder, Colorado: Geological Society of America. https://doi.org/10.1130/dnag-gna-g1.589

Monger, J. W. H., Price, R. A., & Tempelman-Kluit, D. J. (1982). Tectonic accretion and the origin of the two major metamorphic and plutonic welts in the Canadian Cordillera. *Geology*, *10*(2), 70. https://doi.org/10.1130/0091-7613(1982)10<70:taatoo>2.0.co;2

Monger, J. W. (2014). Logan Medallist 1. Seeking the suture: The Coast-Cascade conundrum. *Geoscience Canada*, *41*, –379. https://doi.org/10.12789/geocanj.2014.41.058

Monger, J. W. H., Heyden, P. V. D., Journeay, J. M., Evenchick, C. A., & Mahoney, J. B. (1994). Jurassic-Cretaceous basins along the Canadian Coast Belt: Their bearing on pre-mid-Cretaceous sinistral displacements. *Geology*, *22*(2), 175. https://doi.org/10.1130/0091-7613(1994)022<0175:jcbatc>2.3.co;2

Morris, R. A., DeBari, S. M., Busby, C., Medynski, S., & Jich, B. R. (2019). Building arc crust: Plutonic to volcanic connections in an extensional oceanic arc, the southern Alisitos arc, Baja California. *Journal of Petrology*, *60*(6), 1195–1228. https://doi.org/10.1093/petrology/egz029

Nokleberg, W. J., Jones, D. L., & Silberling, N. J. (1985). Origin and tectonic evolution of the Maclaren and Wrangellia terranes, eastern Alaska Range, Alaska. *Geological Society of America Bulletin*, *96*(10), 1251. https://doi.org/10.1130/0016-7606(1985)96<1251:oateot>2.0.co;2

Nokleberg, W. J., Plafker, G., & Wilson, F. H. (1994). Geology of south-central Alaska. In G. Plafker, & H. C. Berg (Eds.), *The geology of Alaska*. (Vol. G-1, pp. 311–365). Boulder, Colorado: Geological Society of America, Geology of North America

Olson, N. H., Dilles, J. H., Kent, A. J. R., & Lang, J. R. (2017). Geochemistry of the Cretaceous Kaskanak batholith and genesis of the Pebble porphyry Cu-Au-Mo deposit, southwest Alaska. *American Mineralogist, Journal of Earth and Planetary Materials*, *102*(8), 1597–1621. https://doi.org/10.2138/am-2017-6053

Pavlis, T. L., Amato, J. M., Trop, J. M., Ridgway, K. D., Roeske, S. M., & Gehrels, G. E. (2019). Evidence for subduction polarity in ancient arcs: Integrating geological and geophysical approaches to decipher the Mesozoic tectonic history of the northern Cordillera. *GSA Today*, *29*(11), 4–10. https://doi.org/10.1130/GSATG402A.1

Pavlis, T. L., Monteverde, D. H., Bowman, J. R., Rubenstone, J. L., & Reason, M. D. (1988). Early Cretaceous near-trench plutonism in southern Alaska: A tonalite-trondhjemite intrusive complex injected during ductile thrusting along the Border Ranges fault system. *Tectonics*, *7*(6), 1179–1199. https://doi.org/10.1029/TC007i006p01179

Pearce, J. A. (1996). A user's guide to basalt discrimination diagrams. In D. A. Wyman (Ed.), *Trace element geochemistry of volcanic rocks: Applications for massive sulphide exploration*. (Vol. 12, pp. 79–113). St. John's, NL: Geological Association of Canada Short Course Notes

Pearce, J. A., & Peate, D. W. (1995). Tectonic implications of the composition of volcanic arc magmas. *Annual Review of Earth and Planetary Sciences Lett*, *23*(1), 251–285. https://doi.org/10.1146/annurev.ea.23.050195.001343

Pearce, J. A., Stern, R. J., Bloomer, S. H., & Fryer, P. (2005). Geochemical mapping of the Mariana arc-basin system: Implications for the nature and distribution of subduction components. *Geochemistry, Geophysics, Geosystems*, *6*, Q07006. https://doi.org/10.1029/2004gc000895

Plafker, G., & Berg, H. C. (1994). Overview of the geology and tectonic evolution of Alaska. In G. Plafker, & H. C. Berg (Eds.), *The geology of Alaska*. (Vol. G-1, pp. 989–1021). Boulder, Colorado: Geological Society of America, The Geology of North America

Preece, S. J. (1997). *Geochemical variation in the <5 Ma Wrangell Volcanic Field, Alaska with an emphasis on the Skookum Creek Volcanic Complex (Ph.D. thesis)*. Oxford, OH: Miami University

Preece, S. J., & Hart, W. K. (2004). Geochemical variations in the <5 Ma Wrangell Volcanic Field, Alaska: Implications for the magmatic and tectonic development of a complex continental arc system. *Tectonophysics*, *392*(1-4), 165–191. https://doi.org/10.1016/j.tecto.2004.04.011

Putirka, K, & Busby, C.J. (2007). The tectonic significance of high K_2O volcanism in the Sierra Nevada, California. *Geology*, *35*(10), 923–926. https://doi.org/10.1130/G23914A.1

Reid, M., Finzel, E., Enkelmann, E., & Mcclelland, W. (2018). Detrital zircon provenance of Upper Jurassic–Upper Cretaceous forearc basin strata on the Insular terranes, south-central Alaska. In R. V. Ingersoll, T. F. Lawton, & S. A. Graham (Eds.), *Tectonics, sedimentary basins, and provenance: A celebration of the career of William R. Dickinson*. (Vol. 540, pp. 1–20). Boulder, CO: Geological Society of America Special Paper. https://doi.org/10.1130/2018.2540(25)

Richter, D. H. (1971). Reconnaissance geologic map and section of the Nabesna A-3 Quadrangle, Alaska: *U.S. Geological Survey Miscellaneous Geologic Investigations Map 655*, 1 sheet, scale 1:63,360

Richter, D. H. (1976). Geologic map of the Nabesna quadrangle, Alaska: *U.S. Geological Survey Miscellaneous Field Studies Map 655-A*, 1 sheet, scale 1:250,000

Richter, D. H., & Jones, D. L. (1973). Reconnaissance geologic map of the Nabesna A-2 Quadrangle, Alaska: *U.S. Geological Survey Miscellaneous Geologic Investigations Map 749*, 1 sheet, scale 1:63,360

Richter, D. H., Lanphere, M. A., & Matson, N. A. (1975). Granitic plutonism and metamorphism, eastern Alaska Range, Alaska. *Geological Society of America Bulletin*, *86*(6), 819–829. https://doi.org/10.1130/0016-7606(1975)86<819:gpamea>2.0.co;2

Ridgway, K. D., Trop, J. M., Nokleberg, W. J., Davidson, C. M., & Eastham, K. R. (2002). Mesozoic and Cenozoic tectonics of the eastern and central Alaska Range: Progressive basin development and deformation in a suture zone. *Geological Society of America Bulletin*, *114*(12), 1480–1504. https://doi.org/10.1130/0016-7606(2002)114<1480:mactot>2.0.co;2

Romero, M. C., Ridgway, K. D., & Gehrels, G. E. (2020). Geology, U-Pb geochronology, and Hf isotope geochemistry across the Mesozoic Alaska Range suture zone (south-central Alaska): Implications for Cordilleran collisional processes. *Tectonics*, *39*, 1–32. https://doi.org/10.1029/2019TC005946

Rubin, C. M., & Saleeby, J. B. (1991). The Gravina Sequence: Remnants of a Mid-Mesozoic oceanic arc in southern southeast Alaska. *Journal of Geophysical Research*, *96*, 14,551–14,568

Rubin, C. M., Saleeby, J. B., Cowan, D. S., Brandon, M. T., & McGroder, M. F. (1990). Regionally extensive mid-Cretaceous west-vergent thrust system in the northwestern Cordillera: Implications for continental-margin tectonism. *Geology*, *18*(3), 276–280. https://doi.org/10.1130/0091-7613(1990)018<0276:REMCWV>2.3.CO;2

Sandy, M. R., & Blodgett, R. B. (1996). *Peregrinella* (Brachiopoda; Rynchonellida) from the Early Cretaceous, Wrangellia terrane, Alaska. In P. Copper, & J. Jin (Eds.), *Brachiopods, Proceedings of the Third International Brachiopod Congress*. (pp. 239–242). Rotterdam/Brookfield: A. A. Balkema

Short, E., Snyder, D. C., Trop, J. M., Hart, W. K., & Layer, P. W. (2005). New findings on Early Cretaceous volcanism within the allochthonous Wrangellia terrane, south-central Alaska: Stratigraphic, geochronologic, and geochemical data from the Chisana Formation, Nutzotin Mountains. *Salt Lake City Annual Meeting, Abs w/Programs*, *37*, 81

Sigloch, K., & Mihalynuk, M. G. (2017). Mantle and geological evidence for a Late Jurassic–Cretaceous suture spanning North America, *Geological Society of America Bulletin*, *129*, 1489–1520, doi: https://doi.org/10.1130/b31529.1

Sigloch, K., & Mihalynuk, M. G. (2013). Intra-oceanic subduction shaped the assembly of Cordilleran North America. *Nature*, *496*(7443), 50–56. https://doi.org/10.1038/nature12019

Smithies, R. H., Van Kranendonk, M. J., & Champion, D. C. (2007). The Mesoarchean emergence of modern-style subduction. *Gondwana Research*, *11*(1-2), 50–68. https://doi.org/10.1016/j.gr.2006.02.001

Snyder, D. C., & Hart, W. K. (2007). The White Mountain granitoid suite: Isotopic constraints on source reservoirs for Cretaceous magmatism within the Wrangellia Terrane. In K. D. Ridgway, J. M. Trop, J. M. G. Glen, & M. O'Neill (Eds.), *Tectonic growth of a collisional continental margin: Crustal evolution of southern Alaska*. (Vol. 431, pp. 379–399). Boulder, CO: Geological Society of America Special Paper. https://doi.org/10.1130/2007.2431(15)

Stamatakos, J. A., Trop, J. M., & Ridgway, K. D. (2001). Late Cretaceous paleogeography of Wrangellia: Paleomagnetism of the MacColl Ridge Formation, southern Alaska, revisited. *Geology*, *29*, 947–950. https://doi.org/10.1130/0091-7613(2001)029<0947:LCPOWP>2.0.CO;2

Stern, R. J. (2010). The anatomy and ontogeny of modern intra-oceanic arc systems, Kusky, T. M., Zhai, M.-G. & Xiao, W. (Eds.), *The evolving continents: Understanding processes of continental growth*, London, UK: Geological Society, London, Special Publications, 338, 7–34, 1. https://doi.org/10.1144/SP338.2

Stowell, H., Green, N. L., & Hooper, R. J. (2000). Geochemistry and tectonic setting of basaltic volcanism, northern Coast Mountains, Southeastern Alaska. In H. H. Stowell, & W. C. McClelland (Eds.), *Tectonics of the Coast Mountains, southeastern Alaska and British Columbia*. (pp. 235–256). Boulder, Colorado: Geological Society of America Special Paper 343

Sun, S., & McDonough, W. F. (1989). Chemical and isotopic systematics of oceanic basalts: Implications for mantle composition and processes. In A. D. Saunders, & M. J. Norry (Eds.), *Magmatism in the ocean basins*, London, UK: Geological Society of London Special Publication (Vol. 42, No. 1 pp. 313–345). https://doi.org/10.1144/GSL.SP.1989.042.01.19

Tibaldi, A., Pasquarè, F., & Tormey, D. (2010). Volcanism in reverse and strike-slip fault settings. In S. Cloetingh, J. Negendank, & International Year of Planet Earth (Eds.), *New frontiers in integrated solid Earth sciences*. (pp. 315–348). Dordrecht: Springer

Tollstrup, D., Gill, J., Kent, A., Prinkey, D., Williams, R., Tamura, Y., Ishizuka, O. (2010). Across-arc geochemical trends in the Izu-Bonin arc: Contributions from the subducting slab, revisited. *Geochemistry, Geophysics, Geosystems*, *11*, Q01X10. https://doi.org/10.1029/2009GC002847

Trop, J. M., Benowitz, J. A., Cole, R., & O'Sullivan, P. (2019). Cretaceous to Miocene magmatism, sedimentation, and exhumation within the Alaska Range suture zone: A reactivated terrane boundary. *Geosphere*, *15*(4), 1066–1101. https://doi.org/10.1130/GES02014.1

Trop, J. M., Benowitz, J. A., Koepp, D., Sunderlin, D., Brueseke, M., Layer, P., & Fitzgerald, P. (2020). Stitch in the ditch: Nutzotin Mountains (Alaska) fluvial strata and a dike record ~117–114 Ma accretion of Wrangellia with western North America and initiation of the Totschunda fault. *Geosphere*, *16*(1), 82–110. https://doi.org/10.1130/GES02127.1

Trop, J. M., & Ridgway, K. D. (2007). Mesozoic and Cenozoic tectonic growth of southern Alaska: A sedimentary basin perspective. In K. D. Ridgway, J. M. Trop, J. M. G. Glen, & M. O'Neill (Eds.), *Tectonic growth of a collisional continental margin: Crustal evolution of southern Alaska*. (Vol. 431, pp. 55–94). Boulder, CO: Geological Society of America Special Paper. https://doi.org/10.1130/2007.2431(04)

Trop, J. M., Ridgway, K. D., Manuszak, J. D., & Layer, P. (2002). Mesozoic sedimentary-basin development on the allochthonous Wrangellia composite terrane, Wrangell Mountains basin, Alaska: A long-term record of terrane migration and arc construction. *Geological Society of America Bulletin*, *114*(6), 693–717. https://doi.org/10.1130/0016-7606(2002)114<0693:msbdot>2.0.co;2

Trop, J. M., Snyder, D., Hart, W. K., & Idleman, B. D. (2012). Miocene basin development and volcanism along a strike-slip to flat-slab subduction transition: Stratigraphy, geochemistry, and geochronology of the central Wrangell volcanic belt, Yakutat-North America collision zone. *Geosphere*, *8*, 805–834

van Der Heyden, P. (1992). A Middle Jurassic to Early Tertiary Andean-Sierran arc model for the Coast Belt of British Columbia. *Tectonics*, *11*(1), 82–97. https://doi.org/10.1029/91tc02183

Vaughan, A. P. M., & Scarrow, J. H. (2003). K-rich mantle metasomatism control of localization and initiation of lithospheric strike-slip faulting. *Terra Nova*, *15*(3), 163–169. https://doi.org/10.1046/j.1365-3121.2003.00485.x

Waldien, T. S., Roeske, S. M., Benowitz, J. A., Allen, W. K., Ridgway, K. D., & O'Sullivan, P. B. (2018). Late Miocene to Quaternary evolution of the McCallum Creek thrust system, Alaska: Insights for range-boundary thrusts in transpressional orogens. *Geosphere*, *14*(6), 2379–2406. https://doi.org/10.1130/ges01676.1

Yokelson, I., Gehrels, G. E., Pecha, M., Giesler, D., White, C., & McClelland, W. C. (2015). U-Pb and Hf isotope analysis of detrital zircons from Mesozoic strata of the Gravina belt, Southeast Alaska. *Tectonics*, *34*, 2052–2066. https://doi.org/10.1002/2015tc003955